PSERC

Detection, Prevention and Mitigation of Cascading Events

Part I of Final Project Report

Power Systems Engineering Research Center

A National Science Foundation
Industry/University Cooperative Research Center
since 1996

Power Systems Engineering Research Center

Detection, Prevention and Mitigation of Cascading Events

Final Project Report

Part I

Report Authors

Mladen Kezunovic
Hongbiao Song, Nan Zhang
Texas A&M University

PSERC Publication 05-59

October 2005

Information about this project

For information about this project contact:

Mladen Kezunovic, Ph.D., P.E.
Eugene E. Webb Professor
Texas A&M University
Department of Electrical Engineering
College Station, TX 77843-3128
Phone: 979-845-7509
Fax: 979-845-9887
Email: kezunov@ee.tamu.edu

Power Systems Engineering Research Center

This is a project report from the Power Systems Engineering Research Center (PSERC). PSERC is a multi-university Center conducting research on challenges facing a restructuring electric power industry and educating the next generation of power engineers. More information about PSERC can be found at the Center's website: http://www.pserc.org.

For additional information, contact:

Power Systems Engineering Research Center
Cornell University
428 Phillips Hall
Ithaca, New York 14853
Phone: 607-255-5601
Fax: 607-255-8871

Notice Concerning Copyright Material

Acknowledgements

The Power Systems Engineering Research Center sponsored the research project titled "Detection, Prevention and Mitigation of Cascading Events." The project began in 2002. This is Part I of the project report. It is the final report of progress at Texas A&M University.

We express our appreciation for the support provided by PSERC's industrial members and by the National Science Foundation under grant NSF EEC-0002917 received under the Industry / University Cooperative Research Center program.

Particular thanks go to Hydro-Quebec, IREQ, MidAmerican Energy, and Entergy for their involvement in the project. The authors also acknowledge Professors Vijay Vittal and Mani Venkatasubramanian of Arizona State University and Washington State University respectively who contributed technical advice and close cooperation to this work. Vijay Vittal is the project leader.

Executive Summary

This research develops and describes new technologies for monitoring and control at the system and local levels. To achieve more reliable operation, power system operators could benefit from new tools that provide an interactive scheme to detect and prevent possible cascading events. The tools are research grade, but have the potential for further development.

For system monitoring and control, the technologies include routine and event-based security analysis, along with security control schemes. Routine security analysis includes vulnerability analysis, and static and dynamic contingency analysis. The security control scheme includes emergency control for expected and unexpected events. The tools incorporate a fast network contribution factor method that addresses single and multiple network parameters variance for steady state analysis and control. For transient stability analysis and control, the new tools use the potential energy boundary surface method and analytical sensitivity of the energy margin. In addition, two indices, the Vulnerability Index and Margin Index, are developed to represent the vulnerability and security margin information for an individual power system element and for the operating condition of the entire system.

The local monitoring and control consists of an advanced real time fault analysis tool and a relay operation monitoring tool. The main technologies used in the local monitoring tool are a neural network based fault detection and classification algorithm, a synchronized sampling based fault location algorithm, and event tree analysis.

The system monitoring and control tool can be installed at control centers. The local monitoring and control tool can be installed at substations. They can work together in an interactive scheme to help detect and prevent possible cascading events.

The test beds used to demonstrate the scheme for detection and prevention of cascading events are the IEEE 14-bus and 39-bus systems, the WECC 9-bus system, and the CenterPoint Energy SKY-STP system.

Table of Contents

Table of Figures

Table of Tables

1. Introduction

1.1 Problem Description

With the advent of deregulation and restructuring power systems are increasingly being operated close to their limits. As the system become more stressed, weak connections, unexpected events, hidden failures in protection system, human errors, and a host of other reasons may cause the system to lose stability and even experience catastrophic failure. When the power system is subjected to large disturbances, and the vulnerability analysis indicates that the system is approaching a potential catastrophic failure, control actions need to be taken to steer the system away from severe consequences, and to limit the extent of the disturbance.

In the project, the problem is studied in three steps:

(1) Detection of Major Disturbances and Protective Relay Operations Leading to Cascading Events.

(2) Wide Area Measurement Based Remedial Action.

(3) Adaptive Islanding with Selective under Frequency Load Shedding.

This report mainly aims at, but is not limited to, Step 1: Detection of Major Disturbances and Protective Relay Operations Leading to Cascading Events.

Power system cascading outage is quite often a complicated phenomenon, which may finally result in a large area blackout. There are many factors contributing to power system cascading outages, such as inadequate understanding of unfolding events, inadequate operational awareness, inadequate tree trimming, relaying problems, bad weather conditions, human errors, etc [12]. No single factor may be the cause of system cascading outage and large area blackout. From the technical side, relaying setting problems and inadequate understanding of unfolding events are two major contributing factors, although neither of them may be the triggering cause. Relaying problems were the contributing factor in almost 70% of the US disturbances from 1984 to 1991 [13]. Relay failure and misoperation during weakened system conditions contribute the most to the cascading outages. Another problem is that power system operators lack sufficient analysis and decision support to take quick corrective actions due to inadequate understanding of unfolding events. This was clearly demonstrated in the August 1996 US Western Coast System Blackout and August 2003 US Northeastern System Blackout [12,14].

How to detect major disturbances and protective relay operations leading to cascading events is very important and urgent for prevention and mitigation of the cascading events. This report gives a detailed description of the solution scheme.

1.2 Literature Review of the Research on Cascading Events

Different research efforts are aimed at understanding and finding ways to prevent cascading events: dynamic and probabilistic study of the cascade model, dynamic decision-event tree analysis, wide area back-up protection expert system, relay hidden

failure analysis, special protection scheme, etc [15-18]. Cascade model study tries to learn the cascading characteristics from the system dynamics, probability, and power system historical data. Dynamic event tree analysis combines the probability and event tree technique for prediction and mitigation of cascading events. It is still very difficult to generate comprehensive event trees due to the complexity and large number of components of the power system. For the wide area back up protection expert system, it is easy to apply it in the radial system, which is not the frequent configuration of the large and complex transmission network. Special protection scheme is hardware based and designed for particular conditions. It is not flexible and cannot adapt to the dynamic changing conditions in the competitive market environment. There are no effective interactive monitoring and control tools developed so far to detect and mitigate the cascading outage.

1.3 New Proposed Approach

This report presents a new interactive system-wide and local monitoring and control scheme for efficiently detecting and preventing cascading outages.

The proposed system-wide monitoring and control tool is intended for installation at the control center. It consists of routine and event-based security analysis. For the routine static and dynamic contingency analysis, contingencies which can lead to an overload condition, voltage problem, angle stability, voltage stability, etc., will be found and taken care of. Either preventive control actions need to be taken to prevent such problems or emergency control needs to be activated if such contingencies have already happened. Vulnerability analysis of operating condition of the whole system and individual element can be implemented as discussed in this paper. Vulnerable elements will be located and their relays need to be closely monitored. The event-based security analysis is triggered when a disturbance occurs. It will indicate whether the emergency control is needed to mitigate the transient stability problem or not.

The local monitoring and control tool is intended for installation at substations. Neural network based fault detection and classification (NNFDC), synchronized sampling based fault location (SSFL), and event tree analysis (ETA) can be combined as an advanced real time fault analysis tool and relay monitoring system as described in this report. This will provide detailed information about disturbances and related relay operations for each substation.

The on-line implementation of the system-wide, and local monitoring and control tools proposed in this report, will follow these steps:

Step 1: Routine vulnerability and security analysis performed by the system tool: (a) decides security level and finds vulnerable elements, and sends monitoring command to the local tool; (b) identifies critical contingencies, and starts associated control schemes to find the control means for those expected events.

Step 2: Local monitoring performed by the local tool: (a) starts analysis when disturbance occurs; (b) if it finds relay misoperation, it makes correction or receives system control command for better control; (c) reports disturbance information and analysis results to the system tool.

Step 3: Event-based security analysis performed by the system tool: (a) if it finds a match with expected event, activates the emergency control; (b) if it does not find a match, analyzes if the system is secure or not; (c) if it is not, finds new emergency control and activates it.

Step 4: Update information and go to Step 1.

1.4 Summary of the Results

Following conclusions can be drawn:

New approach to detect and prevent cascading outage can be obtained by coordinated the system-wide and local monitoring and control tools.

The system-wide monitoring and control tool can find the vulnerable elements and send request to the local tool for detailed monitoring. The vulnerability and security margin information can be obtained by Vulnerability Index (VI) and Margin Index (MI). Emergency control approaches for expected events can be found by the routine security analysis and activated when such events occur. Emergency control approaches for unexpected events can be found by event-based security analysis and activated to mitigate the disturbance and keep the system secure.

The local monitoring and control tool can find the exact disturbance information and make a correction if there is relay misoperation. Further information can be sent to the system-wide monitoring and control tool for better security control.

1.5 Organization of the Report

The report is organized into five chapters. Chapter one gives the introduction of cascading events, current research efforts on cascading events, approach proposed in this report, summary of results, etc. Chapter two presents the developed techniques for the system-wide monitoring and control tool, including Network Contribution Factor (NCF) method, Vulnerability Index (VI), Margin Index (MI), contingency analysis (CA), steady state analysis and control (SSAC), transient stability analysis and control (TSAC), static and dynamic relay analysis (RA), etc. Chapter three addresses the local monitoring and control tool. The neural network based fault detection and classification (NNFDC), synchronized sampling based fault location (SSFL), and event tree analysis (ETA) combine together into an advanced real time fault analysis tool and relay monitoring tool. Power swing and its influence on the fault analysis are presented. Implementation of simulations is also given. Chapter four presents the interactive scheme between system-wide and local monitoring and control tools to detect and prevent cascading events. How the system-wide as well as local monitoring and control tools work together is described using a block diagram. Numerical results are obtained from the IEEE standard test systems. Chapter five contains conclusions about the techniques and tools studied in this report.

2. The System-Wide Monitoring and Control Tool

2.1 Introduction

The system monitoring and control tool includes methods of network contribution factor (NCF), generator contribution factor (GCF), load contribution factor (LCF), vulnerability index (VI), margin index (MI), potential energy boundary surface (PEBS), analytical sensitivity of transient energy margin, static and dynamic relay analysis (RA), etc. It performs the system-wide routine and event-based security analysis, which include vulnerability analysis (VA), contingency analysis (CA), as well as the steady state control (SSC) and transient stability control (TSC) for expected and unexpected events. The system-wide monitoring and control tool can work together with local monitoring and control tool to help detect and prevent cascading outages, which is described in Chapter 5.

2.2 Network Contribution Factor (NCF) Method

Network Contribution Factor (NCF) method has been developed to analyze the influence on branch flow and bus voltage due to power system network parameter variance. Thus it can give good guidance for solving steady state overload and low voltage problems without many trials of running the load flow. It finds the most contributing parameter variance which can relieve the line overload or improve the bus voltage by using the base flow condition and network information. Line on/off switching, line parameter change due to TCSC insertion, bus shunt capacitor/reactor on/off switching, can all be considered. Not only single parameter but also multi-parameter analysis and control can be achieved. Final results are verified by the full AC load flow. NCF method is demonstrated to be fast and accurate.

The following is the description of the NCF method. Given an n-bus-l-branch system, A is the node-branch incidence matrix, Y_p is the primitive branch admittance matrix, Y_{bs} is the node shunt capacitance matrix,

$$Y_p = diag\begin{bmatrix} y_1 & \dots & y_l \end{bmatrix} \tag{2.1}$$

$$Y_{bs} = diag\begin{bmatrix} y_{s1} & \dots & y_{sn} \end{bmatrix} \tag{2.2}$$

$$A_{ij} = \begin{cases} 1 & \text{i is the sending node of branch j} \\ -1 & \text{i is the receiving node of branch j} \\ 0 & else \end{cases} \tag{2.3}$$

2.3 Real Power Flow Change due to Branch Parameter Variance

From the fast decouple power flow (FDPF), we know the approximate real power equation,

$$\frac{P}{E} = B'\theta \tag{2.4}$$

where P, E, θ are the node real power injection, magnitude and angle of the bus voltage respectively. Assign

$$Y_1 = -imag(Y_p) \tag{2.5}$$

Approximate the line real power flow,

$$P_{line} \cong Y_1 A^T (E\theta) \tag{2.6}$$

Node real power injection is,

$$P_{node} \cong AP_{line} \tag{2.7}$$

Bus voltage angle variance due to line parameter variance,

$$\Delta\theta = -(A(Y_1 + \Delta Y_1)A^T)^{-1}(A\Delta Y_1 A^T)\theta \tag{2.8}$$

Rewrite as

$$\Delta\theta = -X_1(A\Delta Y_1 A^T)\theta \tag{2.9}$$

where

$$X_1 = (A(Y_1 + \Delta Y_1)A^T)^{-1} \tag{2.10}$$

For single parameter variance,

$$\Delta Y_1 = diag[0 \quad .. \quad \Delta y_i \quad .. \quad 0] \tag{2.11}$$

For multi-parameter variance, here only assume at line “i” and “j”, more variances are similar,

$$\Delta Y_1 = diag[0 \quad .. \quad \Delta y_i \quad .. \quad \Delta y_j \quad .. \quad 0] \tag{2.12}$$

Line real power flow variance,

$$\Delta P_{line} = \Delta Y_1 A^T (E\theta) + (Y_1 + \Delta Y_1)A^T (E\Delta\theta) \quad ` \tag{2.13}$$

For single line “i” parameter variance,

(a) For the line “k”, $k \neq i$, real power flow change,

$$\Delta P_{line-k} = -[A_{1k} \quad ... \quad A_{nk}]X_1 K_i (y_k \Delta y_i) \tag{2.14}$$

where

$$K_i = [A_{1i} \quad .. \quad A_{ii} \quad .. \quad A_{ni}]^T \sum_{j=1}^{n} A_{ji} E_j \theta_j \tag{2.15}$$

(b) For the line "i" real power flow change,

$$\Delta P_{line-i} = (\sum_{j=1}^{n} A_{ji} E_j \theta_j / y_i^{'} - [A_{1i} \quad ... \quad A_{ni}] X_1 K_i)(y_i^{'} \Delta y_i) \tag{2.16}$$

For single line outage, simply assign

$$\Delta P_{line-i} = -P_{line-i} \tag{2.17}$$

For multi-parameter variance, assume line "i", "j" for simple example,

(a) For line "k", $k \neq i, j$, real power flow change,

$$\Delta P_{line-k} = -[A_{1k} \quad ... \quad A_{nk}] X_1 (K_i \Delta y_i + K_j \Delta y_j) y_k \tag{2.18}$$

where

$$K_i = [A_{1i} \quad .. \quad A_{ii} \quad .. \quad A_{ni}]^T \sum_{l=1}^{n} A_{li} E_l \theta_l \tag{2.19}$$

$$K_j = [A_{1j} \quad .. \quad A_{jj} \quad .. \quad A_{nj}]^T \sum_{l=1}^{n} A_{lj} E_l \theta_l \tag{2.20}$$

(b) For the line "i", "j" real power flow change,

$$\Delta P_{line-i} = \sum_{l=1}^{n} A_{li} E_l \theta_l (\Delta y_i) - [A_{1i} \quad ... \quad A_{ni}] X_1 (K_i \Delta y_i + K_j \Delta y_j) y_i \tag{2.21}$$

$$\Delta P_{line-j} = \sum_{l=1}^{n} A_{lj} E_l \theta_l (\Delta y_j) - [A_{1j} \quad ... \quad A_{nj}] X_1 (K_i \Delta y_i + K_j \Delta y_j) y_j \tag{2.22}$$

For lines "i", "j" outages, simply assign

$$\Delta P_{line-i} = -P_{line-i} \tag{2.23}$$

$$\Delta P_{line-j} = -P_{line-j} \tag{2.24}$$

2.4 Bus Voltage Change due to Bus Parameter Variance

By the fast decoupled power flow (FDPF),

$$\frac{\Delta Q}{E} = B^{"} \Delta E \tag{2.25}$$

$$\Delta E = (B^{"})^{-1} \frac{\Delta Q}{E} = X_2 \Delta B_s E \tag{2.26}$$

where

$$X_2 = (B^{"})^{-1} \tag{2.27}$$

$$\Delta Q = \Delta B_s E^2 \tag{2.28}$$

For single bus parameter variance at bus "i",

$$\Delta B_s = [0 \quad .. \quad \Delta y_{bs,i} \quad .. \quad 0]^T \tag{2.29}$$

bus "k" voltage variance,

$$\Delta E_k = X_{2,ki} E_k \Delta y_{bs,i} \tag{2.30}$$

For bus multi-parameter variance at bus "i", "j"

$$\Delta B_s = [0 \quad .. \quad \Delta y_{bs,i} \quad .. \quad \Delta y_{bs,j} \quad .. \quad 0]^T \tag{2.31}$$

bus "k" voltage variance,

$$\Delta E_k = X_{2,ki} E_k \Delta y_{bs,i} + X_{2,kj} E_k \Delta y_{bs,j} \tag{2.32}$$

2.5 Flow and Voltage Network Contribution Factor (FNCF and VNCF)

For single line "i" parameter variance,

$$\Delta P_{f,k} = N_{f,k} y_k \Delta y_i \tag{2.33}$$

Flow Network Contribution Factor (FNCF),

For line "k", $k \neq i$

$$N_{f,k} = -[A_{1k} \quad ... \quad A_{nk}] X_1 K_i \tag{2.34}$$

For line "k", $k = i$

$$N_{f,k} = \sum_{j=1}^{n} A_{ji} E_j \theta_j / y_i - [A_{1i} \quad ... \quad A_{ni}] X_1 K_i \tag{2.35}$$

For single bus "i" parameter variance,

$$\Delta E_k = N_{v,ki} E_k \Delta y_{bs,i} \tag{2.36}$$

Voltage Network Contribution Factor (VNCF),

for bus "k",

$$N_{v,ki} = X_{2,ki} \tag{2.37}$$

where

$$K_i \, , X_1 \, , X_2 \text{ in (2.15),(2.10),(2.27).}$$

for fast approximation, we can use base network matrix

$$X_1 = (AY_1 A^T)^{-1} \tag{2.38}$$

For multi-parameter variance, here only take 2 parameters variance as simple example,

For line "i", "j" parameter variance,

$$\Delta P_{f,k} = N_{f,k} y_k K_i (\Delta y_i + \frac{K_j}{K_i} \Delta y_j) \tag{2.39}$$

For bus "i", "j" parameter variance,

$$\Delta E_k = N_{v,ki} E_k \Delta y_{bs,i} + N_{v,kj} E_k \Delta y_{bs,j} \tag{2.40}$$

2.6 System Vulnerability and Security Analysis

This report presents the comprehensive concept of Vulnerability Index (VI) as well as Margin Index (MI) to give precise vulnerability and margin information for individual system element and the whole system-wide performance. At the generator part, vulnerability indices for real power output, reactive power output and generation loss and margin indices for real and reactive power outputs will be given. At the bus part, vulnerability indices for bus voltage performance, loadability and load loss and margin indices for bus voltage performance and loadability will be presented. Islanding and isolated buses due to the line outages will be considered in the load loss part. At the transmission line part, vulnerability indices for line real power, reactive power, line charging, line bus voltage angle difference, line distance relay performance, and line-off influence will be given. The margin indices for line flow, line bus voltage angle

difference and line distance relay are also given. Different weights of different elements will be considered based on their importance and power system operating practice.

Vulnerability Index (VI) and Margin Index (MI) are a good way to assess the vulnerability and security margin of individual element and the whole system. Given a system with "m" generators, "n" buses, "p" lines and "q" loads, we define the comprehensive Vulnerability Index (VI) and Margin Index (MI) sets below.

2.6.1 Vulnerability Index and Margin Index for Generators

$$VI_{Pg,i} = \frac{W_{Pg,i}}{2N}\left(\frac{Pg_i}{Pg_{i,\max}}\right)^{2N} \tag{2.41}$$

$$VI_{Qg,i} = \frac{W_{Qg,i}}{2N}\left(\frac{Qg_i}{Qg_{i,\max}}\right)^{2N} \tag{2.42}$$

$$VI_{gen\_loss,i} = W_{gen\_loss,i}k_i \tag{2.43}$$

$$VI_{gen} = \sum_{i=1}^{m}(VI_{Pg,i} + VI_{Qg,i} + VI_{gen\_loss,i}) \tag{2.44}$$

$$MI_{Pg,i} = 1 - \frac{Pg_i}{Pg_{i,\max}} \tag{2.45}$$

$$MI_{Qg,i} = 1 - \frac{Qg_i}{Qg_{i,\max}} \tag{2.46}$$

where

$VI_{Pg,i}$: *VI* of individual generator real power output

$VI_{Qg,i}$: *VI* of individual generator reactive power output

$VI_{gen\_loss,i}$: *VI* of individual generator loss

VI_{gen}: total *VI* of all generators

$MI_{Pg,i}$: *MI* of individual generator real power output

$MI_{Qg,i}$: M*I* of individual generator reactive power output

$W_{Pg,i}$: weight of individual generator real power output

$W_{Qg,i}$: weight of individual generator reactive power output

$W_{gen\_loss,i}$: weight of individual generator loss influence

Pg_i , Qg_i: individual generator real, reactive power output

$Pg_{i,\max}$: maximum real power output of generator

$Qg_{i,\max}$: maximum reactive power output of generator when Qg_i is positive; minimum

reactive power output of generator when Qg_i is negative

k_i : 1 when generator is off, 0 when generator is on

N: 1 in general

Different weights are chosen based on the system operating practice. For example, large capacity generators and important reactive power supply generators in the load area can be assigned larger values of $W_{gen\_loss,i}$.

2.6.2 Vulnerability Index and Margin Index for Buses

$$VI_{V,i} = \frac{W_{V,i}}{2N}\left(\frac{V_i - V_i^{sche}}{\Delta V_{i,\lim}}\right)^{2N} \tag{2.47}$$

$$VI_{Loadab,i} = \frac{W_{Loadab,i}}{2N}\left(r_{Loadab,i}\right)^{2N} \tag{2.48}$$

$$VI_{load\_loss,i} = W_{load\_loss,i} r_i \tag{2.49}$$

$$VI_{bus} = \sum_{i=1}^{n}\left(VI_{V,i} + VI_{Loadab,i} + VI_{load\_loss,i}\right) \tag{2.50}$$

$$MI_{V,i} = 1 - \left|\frac{V_i - V_i^{sche}}{\Delta V_{i,\lim}}\right| \tag{2.51}$$

$$MI_{Loadab,i} = 1 - r_{Loadab,i} \tag{2.52}$$

where

$VI_{V,i}$: *VI* of individual bus voltage magnitude

$VI_{Loadab,i}$: *VI* of individual load bus loadbility

$VI_{load\_loss,i}$: *VI* of individual load bus load loss

VI_{bus} : total *VI* of all buses

$MI_{V,i}$: *MI* of individual bus voltage magnitude

positive if bus voltage is within limit; zero or negative if it is at or out of the limit

$MI_{Loadab,i}$: *MI* of individual load bus loadbility

$W_{V,i}$: weight of individual bus voltage influence

$W_{Loadab,i}$: weight of individual bus loadability

$W_{load\_loss,i}$: weight of individual bus load loss influence

$r_{Loadab,i}$: bus loadability

$r_{Loadab,i} = \frac{Z_{th,i}}{Z_{L0,i}}$

$Z_{th,i}$: Thevenin equivalent system impedance

$Z_{L0,i}$: equivalent load impedance at steady state

V_i : bus voltage magnitude

V_i^{sche} : scheduled bus voltage magnitude

$\Delta V_{i,\lim}$: voltage variance limit

r_i : load loss ratio, 0~1, 0: no loss; 1: completely loss

N: 1 in general

In this method, loadability is considered by using Thevenin equivalent impedance method [19]. There are other loadability analysis methods which the user can also choose based on their own decision.

2.6.3 Vulnerability Index and Margin Index for Branches

$$VI_{Pf,i} = \frac{W_{Pf,i}}{2N}\left(\frac{Pf_i}{S_{i,\max}}\right)^{2N} \tag{2.53}$$

$$VI_{Qf,i} = \frac{W_{Qf,i}}{2N}\left(\frac{Qf_i}{S_{i,\max}}\right)^{2N} \tag{2.54}$$

$$VI_{Qc,i} = \frac{W_{Qc,i}}{2N}\left(\frac{Qc_i}{Q_{\Sigma}}\right)^{2N} \tag{2.55}$$

$$VI_{line\_ang,i} = \frac{W_{line\_ang,i}}{2N}\left(\frac{La_i}{La_{i,\max}}\right)^{2N} \tag{2.56}$$

$$VI_{\mathrm{Re}lay,i} = \frac{W_{\mathrm{Re}lay,i}}{2N}\left((1/d_{sr,i})^{2N} + (1/d_{rs,i})^{2N}\right) \tag{2.57}$$

$$VI_{line\_off,i} = W_{line\_off,i}k_i \tag{2.58}$$

$$VI_{line} = \sum_{i=1}^{p}\left(VI_{Pf,i} + VI_{Qf,i} + VI_{Qc,i} + VI_{line\_ang,i} + VI_{\mathrm{Re}lay,i} + VI_{line\_off,i}\right) \tag{2.59}$$

$$MI_{Sf,i} = 1 - \frac{Sf_i}{S_{i,\max}} \tag{2.60}$$

$$MI_{line\_ang,i} = 1 - \frac{La_i}{La_{i,\max}} \tag{2.61}$$

$$MI_{\mathrm{Re}lay,i,sr} = d_{sr,i} - K_z\left|\sin(\pi/2 - \alpha + \theta_{d,sr})\right| \tag{2.62}$$

$$MI_{\mathrm{Re}lay,i,rs} = d_{rs,i} - K_z \,|\sin(\pi/2 - \alpha + \theta_{d,rs})| \tag{2.63}$$

where

$VI_{Pf,i}$: *VI* of individual line real power

$VI_{Qf,i}$: *VI* of individual line reactive power

$VI_{Qc,i}$: *VI* of individual line charging

$VI_{line\_ang,i}$: *VI* of individual bus voltage angle difference at each line

$VI_{\mathrm{Re}lay,i}$: *VI* of individual line distance relay

$VI_{line\_off,i}$: *VI* of individual line outage influence

VI_{line} : total *VI* of all lines

$MI_{Sf,i}$: *MI* of individual line flow

$MI_{line\_ang,i}$: *MI* of individual bus voltage angle difference

$MI_{\mathrm{Re}lay,i,sr}$, $MI_{\mathrm{Re}lay,i,rs}$: *MI* of individual line distance relay at sending and receiving ends, defined as the distance from apparent impedance seen by distance relay to relay protection zone circle, zero or negative values mean at or within the protection zone circle

$W_{Pf,i}$: weight of individual line real power influence

$W_{Qf,i}$: weight of individual line reactive power influence

$W_{Qc,i}$: weight of individual line charging influence

$W_{line\_ang,i}$: weight of individual line bus angle difference

$W_{\mathrm{Re}lay,i}$: weight of individual line distance relay

$W_{line\_off,i}$: weight of individual line off influence

Pf_i , Qf_i , Sf_i : line real, reactive and apparent power

$S_{i,\max}$: individual line transmission limit, which can be either thermal limit or transfer limit due to security constraints

Qc_i : individual line charging

Q_Σ : total reactive power output of all generators, or total reactive power of the whole system

La_i : individual bus voltage angle difference at each line

$La_{i,\max}$: bus voltage angle difference limit at each line

$d_{sr,i}$, $\theta_{d,sr}$: magnitude and angle of normalized apparent impedance seen by distance relay from the sending end to receiving end of that line

$d_{rs,i}$, $\theta_{d,rs}$: magnitude and angle of normalized apparent impedance seen by distance relay from the receiving end to sending end of that line

α : line impedance angle

K_z : zone setting, i.e., define 2.4 as zone 3 setting

k_i : 1 when line is off, 0 when line is on.

In this model, the line charging influence is considered for vulnerability index. Some lightly loaded lines and lines with high charging capacitance may contribute much to the reactive power supply and voltage support. Their outages may decrease the reactive power supply or need for generators to generate more reactive power.

The bus voltage angle difference at each line is also an important signal which was ignored in study of others. For example, from the simplest lossless series line model (without charging capacitance), we know that larger bus voltage angle difference means larger power transfer through that line and smaller normalized apparent impedance seen by the line distance relay. Therefore, the line distance relay may misoperate during the overload and low voltage conditions.

For the apparent impedance seen by the line distance relay, if we use the series line model, we can find that normalized apparent impedance is only associated with the bus voltages along the line.

$$Z_{d,sr} = \frac{V_s}{I_{sr}} = \frac{V_s}{(V_s - V_r)/Z_{sr}} \tag{2.64}$$

$$\bar{Z}_{d,sr} = \frac{Z_{d,sr}}{Z_{sr}} = \frac{V_s}{V_s - V_r} = \frac{|V_s|}{|V_s - V_r|}\angle\theta_{d,sr} = d_{sr}\angle\theta_{d,sr} \tag{2.65}$$

For the more accurate Π line model, we can use accurate parameters to calculate the normalized apparent impedance. The smaller the normalized apparent impedance seen by distance relay at no fault condition, the more possible the case that it may fall into the distance relay backup zone (zone 3 or zone 2 taken as backup). The smaller the apparent impedance, the more vulnerable the distance relay and the smaller the relay margin.

The aggregate system Vulnerability Index (*VI*) can be presented by

$$VI = W_{gen}VI_{gen} + W_{bus}VI_{bus} + W_{line}VI_{line} \tag{2.66}$$

This leads to the following conclusion: the larger the *VI* value, the more vulnerable the system condition.

From different *VI* and *MI* values for various system conditions, we can know more about the whole system vulnerability and security as well as the performance of individual system elements.

2.7 Transient Stability Analysis

2.7.1 Time Domain Method

Time domain method is the most popular and accurate method in transient stability analysis [20]. It uses a step-by-step method to solve the differential and algebraic equations of the power system during the whole simulation period, pre-fault, during-fault, and post-fault. It can use the most detailed system model and normally is taken as the

benchmark for other methods because of its highest accuracy. The angle criterion can be used to judge whether the system is stable or not after the whole simulation period, for example, maximum absolute angle smaller than 2π, or maximum angle difference smaller than π.

The simplest machine model for transient stability analysis is the classical model, as described in the following example with "n" generators and "m" buses:

Two differential equations for each machine:

$$\frac{d\delta}{dt} = \omega - \omega_s \tag{2.67}$$

$$\frac{2H}{\omega_S}\frac{d\omega}{dt} = P_M - P_D - P_i \tag{2.68}$$

One complex power balance equation (two real equations) for each bus of the network:

$$I = YV \tag{2.69}$$

One complex equation (two real equations) for the interface between each generator and network.

$$E' - (R_s + jX'_d)I_t = V_t \tag{2.70}$$

Therefore, the total equations for the system are:

- $2n$ differential equations
- $2(n+m)+2n$ real algebraic equations.

There are more detailed machine model, for example, one axis model (described by 4 differential equations), two-axis model (described by 7 differential equations), which can give more accurate simulation results but need more simulation time.

2.7.2 PEBS Method

By using Lyapunov second or direct criterion, direct methods replace the numerical integration of the post-fault equations by a stability criterion [21,22]. They view the system operating point as a stable equilibrium point that is surrounded by a region in the state space, called the region of stability. If the power system is initialized inside the region of stability, the system will eventually return to the stable operating point. Normally they use the classical model of generators, use either reduced or structure-preserving network, constant impedance model or voltage dependent model to analyze transient stability and voltage problems.

In the Center of Angle (COA) reference,

$$\dot{\theta}_i = \tilde{\omega}_i \tag{2.71}$$

$$M_i \dot{\tilde{\omega}}_i = P_i - P_{ei} - \frac{M_i}{M_T} P_{COI} \tag{2.72}$$

where

$$P_{ei} = \sum_{j=1, j\neq i}^{n} [C_{ij} \sin(\theta_i - \theta_j) + D_{ij} \cos(\theta_i - \theta_j)] \tag{2.73}$$

$$P_i = P_{mi} - E_i^2 G_{ii} \tag{2.74}$$

$$P_{COI} = \sum_{i=1}^{n} (P_i - P_{ei}) \tag{2.75}$$

$$M_T = \sum_{i=1}^{n} M_i \tag{2.76}$$

$$C_{ij} = E_i E_j B_{ij} \tag{2.77}$$

$$D_{ij} = E_i E_j G_{ij} \tag{2.78}$$

Cij, Dij: real and reactive parts of the admittance matrix. They change during conditions of pre-, during, and post-fault.

By linear path-dependence assumption, we can get the transient energy function as following,

$$V(\theta, \tilde{\omega}) = V_{KE} + V_{PE} \tag{2.79}$$

where

$$V_{KE} = \frac{1}{2} \sum_{i=1}^{n} M_i \tilde{\omega}_i^2 \tag{2.80}$$

$$V_{PE} = -\sum_{i=1}^{n} P_i^{pf} (\theta_i - \theta_i^s) - \sum_{i=1}^{n-1} \sum_{j=i+1}^{n} [C_{ij}^{pf} (\cos\theta_{ij} - \cos\theta_{ij}^s) - \beta_{ij} D_{ij}^{pf} (\sin\theta_{ij} - \sin\theta_{ij}^s)] \tag{2.81}$$

As for the transient angle stability, transient energy margin can be calculated by following equation:

$$\Delta V = V(\theta^u, \tilde{\omega}^u) - V(\theta^{cl}, \tilde{\omega}^{cl}) \tag{2.82}$$

Since at UEP, $\tilde{\omega}^u = 0$, we can get

$$\Delta V = -\frac{1}{2}\sum_{i=1}^{n} M_i \tilde{\omega}_i^{cl^2} - \sum_{i=1}^{n} P_i^{pf}(\theta_i^u - \theta_i^{cl}) - \sum_{i=1}^{n-1}\sum_{j=i+1}^{n}[C_{ij}^{pf}(\cos\theta_{ij}^u - \cos\theta_{ij}^{cl}) - \beta_{ij} D_{ij}^{pf}(\sin\theta_{ij}^u - \sin\theta_{ij}^{cl})] \quad (2.83)$$

where

$$\beta_{ij} = \frac{\theta_i^u + \theta_j^u - \theta_i^s - \theta_i^s}{\theta_{ij}^u - \theta_{ij}^s} \text{ (linear dependence direction)} \quad (2.84)$$

θ^{cl} : rotor angle positions at the end of disturbance
$\tilde{\omega}^{cl}$: velocities at the end of disturbance
θ^u : controlling u.e.p (unstable equilibrium point)

Direct methods fall into finding the controlling unstable equilibrium point (UEP), ($\theta^u, \tilde{\omega}^u$), at which point, the system loses its stability. However, it is not an easy job to find the controlling UEP.

Potential Energy Boundary Surface (PEBS) method is a fast direct method, which does not need the time consuming controlling (UEP) calculation [21]. It is based on physical intuition. Its procedure is: from the post-fault SEP first draw a number of rays in every direction in the angle space with COA as reference. Along each ray, search for the first point where the potential part of the Lyapunov energy function attains its relative maximum. The points of δs are thus obtained and these rays are then joined to form the boundary surface of interest (stability boundary). This characterizes the PEBS. Mathematically, PEBS crossing can be obtained by setting the directional derivative (along the rays emanating from stable equilibrium point (SEP)) of $V_P(\theta)$ to zero, as follows:

$$[f(\theta)]^T \bullet (\theta - \theta^s) = 0 \quad (2.85)$$

$$i.e., \sum_{i=1}^{n} f_i(\theta)(\theta_i - \theta_i^s) = 0$$

where

$$f_i(\theta) = -\frac{\partial V_{PE}(\theta)}{\partial \theta_i} = P_i - P_{ei} - \frac{M_i}{M_T} P_{COI} \text{ (use the post-fault configuration)} \quad (2.86)$$

Inside the PEBS the $[f(\theta)]^T \bullet (\theta - \theta^s)$ is smaller than 0 and outside the PEBS it is larger than 0. So $[f(\theta)]^T \bullet (\theta - \theta^s)$ change sign from '-' to '+' is the indication of PEBS crossing.

PEBS method assumes that the system critical energy value is equal to the system potential energy maximum value along the system trajectory.

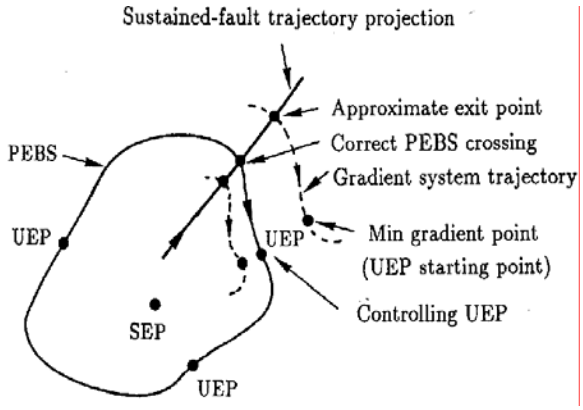

Figure 2.1 PEBS crossing and controlling UEP

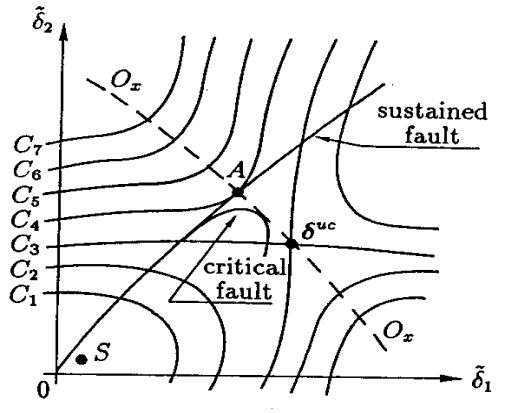

Figure 2.2 System trajectory in the rotor angle space

We can see from Figure 2.1 and Figure 2.2 that when the system is not very ill-conditioned, the controlling UEP, and the PEBS crossing points of fault-on and critical trajectories are very close. Therefore, PEBS method can get an accurate approximation of critical clearing time (CCT). The advantage of PEBS method is that it does not need the Controlling UEP calculation, which is very complex and time consuming. The system post-fault trajectory path is not known before the CCT solution. It may give either an optimistic or pessimistic estimate of the CCT. Iterative PEBS and Corrective PEBS are proposed to give more accurate solution of CCT [22,23].

Step 1, integrate the fault-on trajectory, use the fault-on δ and post-fault Y matrix to get the first PEBS crossing point δ_{cross}, that is, at time T, post fault $[f(\theta)]^T \bullet (\theta - \theta^s)$ changes the sign from '-' to '+', and potential energy V_{PE} gets its local maximum which is the first estimate of Vcr.

Step 2, use the fault-on δ, ω and fault-on Y matrix to find the total transient energy V equal to V_{PE}. That time point Tu is the estimate of the CCT.

Step 3, integrate the post-fault trajectory from time Tu to T.

Step 4, if $[f(\theta)]^T \bullet (\theta - \theta^s)$ doesn't change the sign, that Tu is the CCT, stop. Else, find the new $V_{PE,max}$ and δ_{cross}, go to Step 2 to find new Tu, say it is Tu2. If $|Tu2 - Tu| \le \varepsilon$, stop, either Tu or Tu2 is the CCT. Else, let Tu=Tu2, go to Step 3.

From this iterative or corrective PEBS method, we can get the more accurate results of the CCT. For the transient energy margin, we can use δ_{cross} as the approximate δ^u, and then use (2.83) to get the energy margin.

2.8 Wide Area Relay Monitoring

2.8.1 Analysis of Static Relay Behavior

For the steady states of pre-fault and post-fault conditions, we can calculate the apparent impedances seen by distance relay from (2.64)-(2.65). Thus we can even find the distance

from apparent impedance to protection zone of the distance relay from (2.62)-(2.63). If the values of the $MI_{\mathrm{Re}lay,sr}$ or $\bar{Z}_{d,sr}$ are too small, it is possible that the distance relay may see fault within its protection zone while in reality it is not.

2.8.2 Analysis of Dynamic Relay Behavior

Transient angle stability analysis studies whether the system can obtain an equilibrium point after a major disturbance. Critical clearing time (CCT) is a popular index. It does not consider too much the relay behavior during transients. However, distance relays may see apparent impedance fall into their protection zones during power swing even though the system is stable from the transient stability viewpoint. Hence, relay dynamic behavior must be considered.

Here we give a simple description of the system dynamic behavior during transient. The algebraic equations for an n-machine, m-bus network are described by

$$\begin{bmatrix} I_g \\ I_l \end{bmatrix} = \begin{bmatrix} Y_{gg} & Y_{gl} \\ Y_{\mathrm{lg}} & Y_{ll} \end{bmatrix} \begin{bmatrix} V_g \\ V_l \end{bmatrix} \tag{2.87}$$

where

V_g , I_g : generator bus voltage phasors and injection current phasors

V_l , I_l : load bus voltage phasors and injection current phasors

We can get the time domain V_g , I_g phasors easily from the machine internal currents and voltages during transient. The Y matrix will change due to the pre-fault, during-fault and post-fault periods. For example, for 2-axis machine model,

$$I_g = I_{Di} + jI_{Qi} = (I_{di} + jI_{qi})e^{j(\delta_i - \pi/2)} \tag{2.88}$$

$$V_g = E'_{Di} + jE'_{Qi} = (E'_{di} + jE'_{qi})e^{j(\delta_i - \pi/2)} \tag{2.89}$$

By assuming constant impedance load model, that is, $I_l = 0$, we can get bus voltage phasors

$$V_l = -(Y_{ll})^{-1} Y_{\mathrm{lg}} V_g \tag{2.90}$$

Thus we can get apparent impedance seen by distance relay

$$\bar{z}_{ij} = \frac{V_i}{I_{ij}} = \frac{V_i}{V_i - V_j} z_{ij} = d_{ij} z_{ij} \tag{2.91}$$

where z_{ij} is the impedance of line i-j.

For the static line distance relay (with mho characteristic), it will operate if

$$\left|\bar{z}_{ij} - \rho\right| \le \left|\rho\right| \tag{2.92}$$

where

$$\rho = \beta z_{ij} / 2 \tag{2.93}$$

Normalize as

$$\left|d_{ij} - \beta/2\right| \le \beta/2 \tag{2.94}$$

For typical relay settings, $\beta = 0.8$ for zone 1, $\beta = 1.2$ for zone 2, zone 3 relay settings are power system dependent; here we choose 2.4.

2.8.3 Topology Processing

For a small size system, one or two line outages may lead to system islanding. Even for a big size system, different control areas may have limited number of tie-lines. If they are disconnected, the whole system may split into several smaller systems and cascading outages may occur in those smaller systems if they are unbalanced. Thus, some critical lines must be identified. The relays on these lines need to be monitored. If they misoperate, system security may be decreased. We use the topology processing method based on the node-branch incidence matrix to find the single line list (for N-1 contingency) and critical line pair list (for N-2 contingency). Their disconnection can isolate one or several buses from the other part of the system.

By performing topology processing, as well as static and dynamic relay analysis, the important or vulnerable relays can be chosen for detailed monitoring and control by the local tool. The techniques of the local monitoring and control tool are described in Chapter 3.

2.9 Steady State Control Scheme

2.9.1 Generator Contribution Factor (GCF) Method

Let the gross nodal power P_i^g flowing through node "i" (when looking at the inflows) be defined by

$$P_i^g = \sum_{j \in \alpha_i^u} \left|P_{ij}^g\right| + P_{Gi} \quad \textit{for } i = 1,2,\ldots,n \tag{2.95}$$

where α_i^u is the set of nodes supplying power and directly connected into node "i", and P_{Gi} is the power generation injected into node "i". Under normal situations, we can rewrite the equation as:

$$P_i^g - \sum_{j \in \alpha_i^u} \frac{\left|P_{ji}^g\right|}{P_j} P_j^g = P_{Gi} \quad or \quad A_u P_{gross} = P_G \tag{2.96}$$

where A_u is the upstream distribution matrix with its (ij)th element defined by

$$[A_u]_{ij} = \begin{cases} 1 & for\ i = j \\ -\left|P_{ji}\right| / P_j & for\ j \in \alpha_i^u \\ 0 & other \end{cases} \tag{2.97}$$

where P_{ji} is the real power flow from node "j" to node "i" in line j-i; P_j is the total real power injected into node "j". Then we have

$$P_i^g = \sum_{k=1}^{n} [A_u^{-1}]_{lk} P_{Gk} \quad for\ i=1,2,\ldots,n \tag{2.98}$$

Finally, the contribution of each generator to line i-j flow can be calculated by

$$P_{ij}^g = \sum_{k=1}^{n} D_{ij,k}^g P_{Gk} \quad for \quad j \in \alpha_i^u \tag{2.99}$$

where $D_{ij,k}^g = P_{ij}^g [A_u^{-1}]_{ik} / P_i^g$ is called the topological generation distribution factor, and the contribution of generator "k" to line i-j is equal to $D_{ij,k}^g P_{Gk}$.

2.9.2 Load Contribution Factor (LCF) Method

Similarly, let the gross nodal power P_i^n (looking from outflows) be defined by

$$P_i^n = \sum_{j \in \alpha_i^d} \left|P_{ij}^n\right| + P_{Li} \quad for\ i = 1,2,\ldots,n \tag{2.100}$$

where α_i^d is the set of nodes supplied directly from node "i", and P_{Li} is the load at node "i". Similarly, we can rewrite the equation as:

$$P_i^n - \sum_{j \in \alpha_i^{du}} \frac{\left|P_{ji}\right|}{P_j} P_j^n = P_{Li} \quad or \quad A_d P_{net} = P_L \tag{2.101}$$

where A_d is the downstream distribution matrix with its (ij)th element defined by

$$[A_d]_{ij} = \begin{cases} 1 & for\ i = j \\ -\left|P_{ji}\right| / P_j & for\ j \in \alpha_i^d \\ 0 & other \end{cases} \tag{2.102}$$

$$P_i^n = \sum_{k=1}^{n} [A_d^{-1}]_{lk} P_{Lk} \quad for\ i=1,2,\ldots,n \tag{2.103}$$

Finally, the contribution of each load to line i-j flow can be calculated by

$$P_{ij}^n = \sum_{k=1}^{n} D_{ij,k}^n P_{Lk} \quad for \ \ j \in \alpha_i^d \tag{2.104}$$

where $D_{ij,k}^n = P_{ij}^n [A_d^{-1}]_{ik} / P_i^n$ is called the topological load distribution factor, and the contribution of load "k" to line i-j is equal to $D_{ij,k}^n P_{Lk}$.

2.9.3 Steady State Control Scheme

The NCF, GCF, and LCF methods can combine into a steady state control scheme. In the electricity market environment, the control objective of this scheme is to minimize the generation variation between the original contract and adjusted amount. When the steady state problem (congestion) occurs, first the network control is used. If it can eliminate the congestion, no other control is needed. If not, check whether load management is available or not. If it is not available, the minimum generator re-dispatching by using generator contribution factor (GCF) is chosen. If load management is available, the generator re-dispatching and load management are combined based on the generator and load contribution information. For the generator re-dispatching, decrease the output of the most congestion-contributing generators and increase the output of the least congestion-contributing generators to balance the load and supply. Then run the power flow to check the result. If the congestion is solved and no other line congestion or voltage violation exists, control command will be issued. If not, go to the associated generator re-dispatching and load management analysis and check with power flow until solving the congestion problem. The flow chart of the control scheme is shown in Figure 2.3.

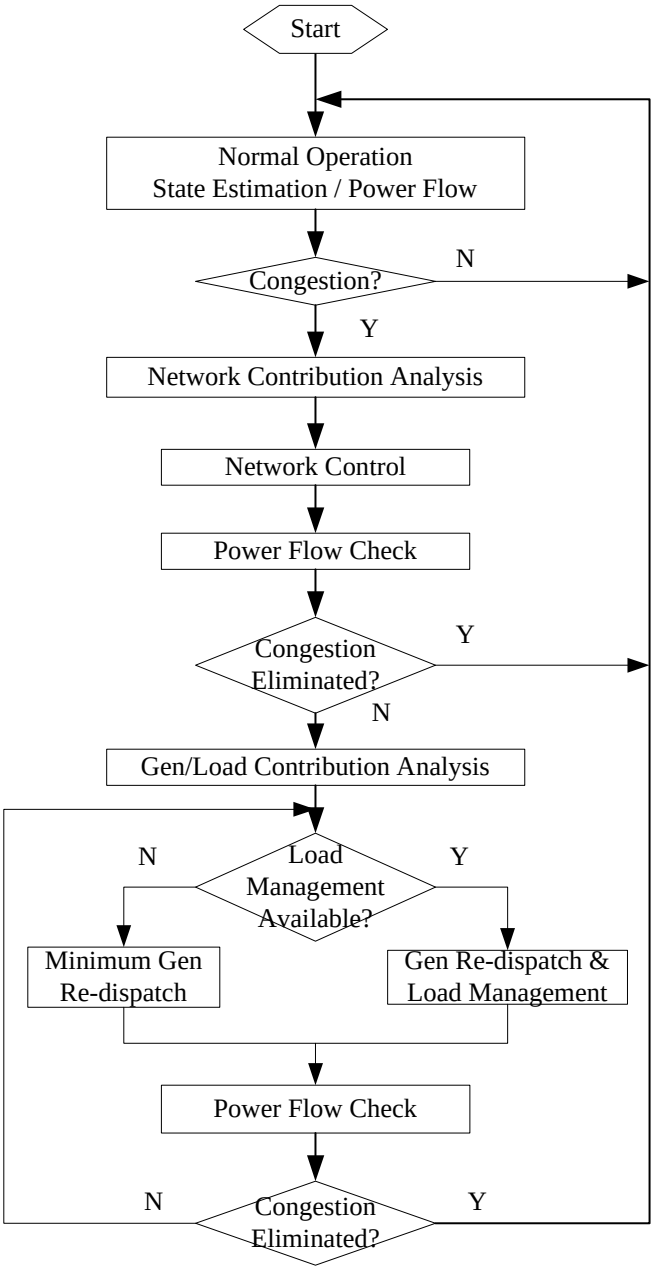

Figure 2.3 Flow chart of steady state control scheme

2.10 Transient Stability Control Scheme

2.10.1 Stability Control Classification

There are many fast stability control means in the literature [20] and real practice. From the generator side, we have the generator tripping, fast valving, dynamic braking, etc. From the load side, we have the load reduction (by voltage reduction), load shedding, etc. From the network side, we have FACTS controllers (TCSC, SVC, etc.), shunt reactors and capacitors, switching on/off lines, etc. For all the above control means, there are two

comprehensive ways: either change the Pm (fast valving), or change the admittance matrix. The generator tripping is the combination of the two. Therefore, we can define two stability control categories, generator-input-based control (GIBC) means, and admittance-based control (ABC) means.

For generator-input-based control (GIBC) means, the variance of Pm can be easily obtained. For admittance-based control (ABC) means, the variances of admittance matrix Y can be obtained as follows:

For a g-generator-l-bus system, the augmented admittance matrix:

$$\hat{Y} = \begin{bmatrix} Y_{gg} & Y_{gl} \\ Y_{\mathrm{lg}} & Y_{ll} \end{bmatrix} \tag{2.105}$$

where

$$Y_{ll} = Y_{bus} + Y_{gen} + Y_{load} \tag{2.106}$$

Y_{bus}: load flow node admittance matrix
Y_{gen}: at generator-connected bus, admittance of generator branch, others, 0
Y_{load}: at load bus, constant admittance of load, others, 0
Y_{ll}: lxl bus admittance matrix
Y_{gg}: gxg generator admittance matrix
Y_{gl}: gxl generator-bus admittance matrix
Y_{lg}: lxg bus-generator admittance matrix

The reduced admittance matrix is:

$$Y = Y_{gg} - Y_{gl}(Y_{ll})^{-1}Y_{\mathrm{lg}} \tag{2.107}$$

For all the single admittance-based control (excluding generator tripping), from fast decoupled power flow method [24], we know that

$$Y_{ll,new} = Y_{ll} - b * M^{T} * M \tag{2.108}$$

$$(Y_{ll,new})^{-1} = (Y_{ll})^{-1} - c * X * M * (Y_{ll})^{-1} \tag{2.109}$$

where

$$c = (-1/b + M * X)^{-1} \tag{2.110}$$

$$X = (Y_{ll})^{-1} * M^{t} \tag{2.111}$$

Therefore, we get the reduced admittance matrix variance for each control means,

$$\Delta Y = Y_{new} - Y_{old} = Y_{gl}[(Y_{ll})^{-1} - (Y_{ll,new})^{-1}]Y_{\mathrm{lg}} = Y_{gl}[cXM(Y_{ll})^{-1}]Y_{\mathrm{lg}} \tag{2.112}$$

There are different network control means to change the reduced admittance matrix as follows:

Case (1). one line i-j outage or switching off

M: row vector which is null except for $M_i = a$ and $M_j = -1$, where a is off-nominal turns ratio referred to the bus corresponding to column "i" for a transformer and $a=1$ for a line

b: line or nominal transformer series admittance

Case (2). one line i-j switching on

M: row vector which is null except for $M_i = -a$ and $M_j = 1$. a, b are the same as above.

Case (3). inserting TCSC at line i-j, compensation k, 0<k<1

M: row vector which is null except for $M_i = a$ and $M_j = -a$, $a = \sqrt{1/k - 1}$. b is the same as above.

Case (4). at bus "i", switching on shunt reactor, capacitor, braking-resistor, SVC

M: row vector which is null except for $M_i = 1$

b: admittance of shunt reactor, capacitor, braking-resistor, SVC

Case (5). at bus "i", switching off shunt reactor, capacitor, braking-resistor, SVC, load reduction

M: row vector which is null except for $M_i = -1$

b: admittance of shunt reactor, capacitor, braking-resistor, SVC. For load reduction or shedding, b=k, $0 \le k \le 1$

2.10.2 Sensitivity Analysis

For the transient energy margin, its sensitivity to a change in any parameter α_k ($\theta^{cl}, \theta^u, \tilde{\omega}^{cl}, P_i^{pf}, B_{ij}^{pf}, G_{ij}^{pf}$), can be given by the partial derivative of ΔV with respective to α_k.

$$\Delta V = \sum_{k=1}^{m} \frac{\partial \Delta V}{\partial \alpha_k} \Delta \alpha_k \tag{2.113}$$

For our control means, since the clearing time is known, we only consider the changes of $\theta^u, P_i^{pf}, B_{ij}^{pf}, G_{ij}^{pf}$. We can get the change of energy margin by

$$\Delta V = \sum_{i=1}^{n} \frac{\partial \Delta V}{\partial P_{mi}} \Delta P_{mi} + \sum_{i=1}^{n} \frac{\partial \Delta V}{\partial G_{ii}} \Delta G_{ii} + \sum_{i=1}^{n-1} \sum_{j=i+1}^{n} \frac{\partial \Delta V}{\partial G_{ij}} \Delta G_{ij} \sum_{i=1}^{n-1} \sum_{j=i+1}^{n} \frac{\partial \Delta V}{\partial B_{ij}} \Delta B_{ij} + \sum_{i=1}^{n} \frac{\partial \Delta V}{\partial \theta_i^u} \Delta \theta_i^u \tag{2.114}$$

where

$$\frac{\partial \Delta V}{\partial P_{mi}} = -(\theta_i^u - \theta_i^{cl}) \tag{2.115}$$

$$\frac{\partial \Delta V}{\partial G_{ii}} = E_i^2(\theta_i^u - \theta_i^{cl}) \tag{2.116}$$

$$\frac{\partial \Delta V}{\partial G_{ij}^{pf}} = \beta_{ij} E_i E_j (\sin\theta_{ij}^u - \sin\theta_{ij}^{cl}) \tag{2.117}$$

$$\frac{\partial \Delta V}{\partial B_{ij}^{pf}} = -E_i E_j (\cos\theta_{ij}^u - \cos\theta_{ij}^{cl}) \tag{2.118}$$

$$\frac{\partial \Delta V}{\partial \theta_i^u} = -P_i^{pf} + \sum_{j=i+1}^{n} (E_i E_j B_{ij}^{pf} \sin\theta_i^u + \beta_{ij} E_i E_j G_{ij}^{pf} \cos\theta_i^u) \tag{2.119}$$

we get the ΔG_{ij} , ΔB_{ij} from (2.112).

For big parameter change (i.e., additional network topology change), controlling UEP may change. From [25] we get

$$(A)(\Delta\theta_i^u) = R_i \tag{2.120}$$

where

$$A_{ii} = (1 - 2\frac{M_i}{M_T}) \sum_{j=1, j\neq i}^{n} C_{ij} \cos\theta_{ij}^u \tag{2.121}$$

$$A_{ij} = (2\frac{M_j}{M_T}) \sum_{l=1, l\neq j}^{n} D_{lj} \sin\theta_{lj}^u + C_{ij} \cos\theta_{ij}^u - D_{ij} \sin\theta_{ij}^u \tag{2.122}$$

$$R_i = E_i^2 \Delta G_{ii} - \frac{M_i}{M_T} \sum_{j=1}^{n} E_j^2 \Delta G_{jj} - \frac{M_i}{M_T} \sum_{l=1}^{n} \sum_{j=1, j\neq l}^{n} E_l E_j \cos\theta_{lj} \Delta G_{lj} + \sum_{j=1, j\neq i}^{n} [E_i E_j \sin\theta_{ij}^u \Delta B_{ij} + E_i E_j \cos\theta_{ij}^u \Delta G_{ij}] \tag{2.123}$$

Therefore, we can get

$$\Delta\theta^u = A^{-1} R \tag{2.124}$$

$$\theta_{i,new}^u = \theta_i^u + \Delta\theta_i^u \tag{2.125}$$

if $\max(\Delta\theta^u) < \varepsilon$, assume controlling UEP does not change, ignore the 5th item of (2.114).

2.10.3 Transient Stability Control Scheme

After a big disturbance (fault) and its clearing, first we do the transient stability study (i.e., use PEBS method) to see if the system is stable or not. If yes, keep monitoring the system. If not, check all available control means being considered or not. If all control means have not been analyzed, use the sensitivity analysis of energy margin to find the suitable control to make the system stable, then check the solution in the transient stability program to make sure it will work. Finally, issue the control command to stabilize the system and keep monitoring the system. If all control means are analyzed and the system is still unstable, warning will be given and the process will stop. In general, as the last defense, load shedding and islanding may be deployed to try to keep the loss as minimal as possible to make the system stable.

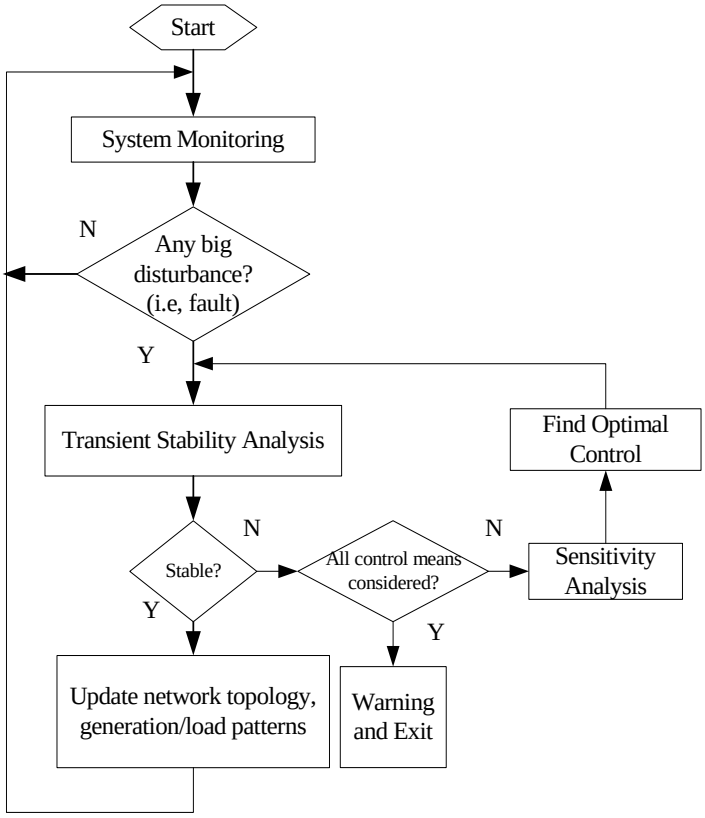

Figure 2.4 Flow chart of the stability control scheme

2.11 Case Studies

Here we give only two study cases for steady state control and transient stability control schemes using a modified IEEE 14-bus system. The load and generation are modified (their values are given in Table 2.1), and transformer branches 5-6, 4-7, 4-9 are changed into transmission lines (with reactance being the same) from the standard IEEE 14 bus system. There is power wheeling from the Area A to the Area B through the tie-lines 5-6, 4-7, 4-9.

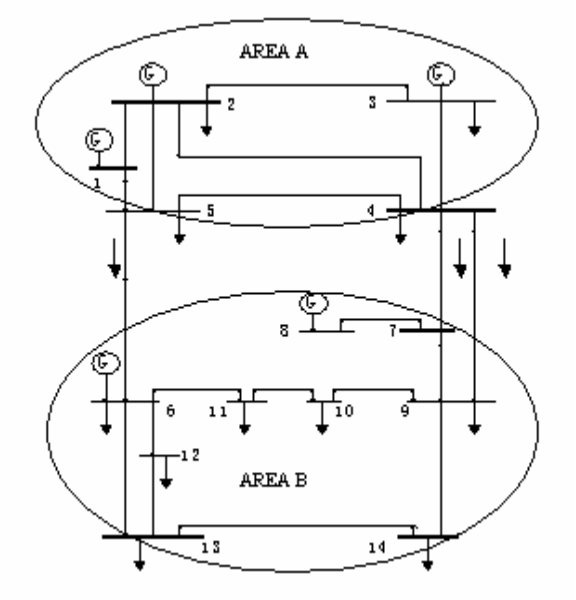

Figure 2.5 Modified IEEE 14-bus system

Table 2.1 Base Flow Condition (Pd, Qd, Bs, Pg: MVA; V: p.u.)

Bus	Pd	Qd	Bs	Pg	V
1	0.00	0.00	0.	232.39	1.060
2	21.70	12.70	0.	65.00	1.045
3	64.20	19.00	0.	65.00	1.010
4	47.80	-3.90	0.	0.00	0.996
5	7.60	1.60	0.	0.00	1.001
6	11.20	7.50	0.	38.00	1.050
7	0.00	0.00	0.	0.00	1.013
8	0.00	0.00	0.	35.00	1.060
9	59.50	16.60	19.	0.00	1.004
10	29.00	5.80	0.	0.00	0.995
11	23.50	1.80	0.	0.00	1.010
12	49.10	1.60	0.	0.00	0.977
13	63.50	5.80	0.	0.00	0.983
14	44.90	5.00	0.	0.00	0.950

Table 2.2 Base Tie-Line Flow (p.u.)

Branch	Real Line flow
1 (bus 5-6)	1.1446
2 (bus 4-7)	0.6156
3 (bus 4-9)	0.4142

Figure 2.5 gives the modified IEEE 14-bus system configuration. Table 2.1 gives the base flow condition. Columns 2 and 3 are real and reactive load at each bus. Column 4 is shunt capacitance at each bus. Column 5 is generator output. Column 6 is bus voltage magnitude in p.u.. Table 2.2 gives the real power flow at each tie-line.

2.11.1 Steady State Control Scheme Case Study

The line 1 flow limit is assumed to be 1 p.u. for security reason. Network control means need to be taken to decrease the power flow at line 1. Here we assume two network control means, inserting Thyristor Controlled Series Capacitor (TCSC) at each line (assume we have a TCSC at each line) and switching off the line. By assuming all the lines have a capability of 50% compensation capacity by TCSC except for line 1, we get the flow network contribution factor FNCF to the line 1 flow variance.

Table 2.3 Flow Network Contribution Factors

Line	Insertion of TCSC	Switch off line
2	-0.0057	-0.0168
3	-0.0152	-0.0212
4	-1.0415e-004	-6.2903e-004
5	-2.0882e-004	-4.8527e-004
6	-8.2135e-004	-0.0013
7	8.1889e-004	0.0014
8	5.9739e-004	9.4764e-004
9	-2.0171e-004	-5.1899e-004
10	-1.7820e-004	-9.1447e-004
11	0.0	PF diverge
12	-0.0023	-0.0128
13	-4.6534e-004	-0.0043
14	1.2026e-004	4.6382e-004
15	4.8069e-004	0.0011
16	7.3215e-004	0.0005
17	-0.0032	-0.0113
18	-0.0011	-0.0042
19	-9.4881e-005	-2.4197e-004
20	-7.6601e-004	-0.0021

From (2.33), when inserting TCSC at each line, $y_k \Delta y_i$ is positive. Negative value of contribution factor represents load flow reduction when the real line flow is in the same direction with defined flow direction. When switching off the line, $y_k \Delta y_i$ is negative. Positive value of contribution factor represents load flow reduction.

From Table 2.3, we know that inserting TCSC at line 3 and switching off line 7 respectively contribute the most to relieving congestion on the line 1. When line 7 is switched off, the real power reduction of line 1 is 0.0235 p.u., which is very close to the power flow result, 0.0202 p.u. When the TCSC compensation is 50% of line 3 reactance, the real power reduction of line 1 is 0.0849 p.u., which is very close to the power flow result, 0.0832 p.u.. We can see that 50% compensation at line 3 is better than switching off line 7 for relieving line 1 congestion. In order to decrease the real power flow at line 1 to 1 p.u., the TCSC compensation capacity should be 68.75% of line 1 reactance.

If we have only 50% compensation capacity and no load management available, we need to re-dispatch the generation. After the 50% compensation at line 3, we have the generator contribution factor table as given in Table 2.4:

Table 2.4 Flow Generator Contribution Factor

Line	Gen 1	Gen 2	Gen 3	Gen 4	Gen 5
1	0.4060	0.2305	0	0	0
2	0.1585	0.2045	0.1451	0	0
3	0.1067	0.1376	0.0977	0	0
4	0.5984	0	0	0	0
5	0.1037	0.1733	0	0	0
6	0.2206	0.3687	0	0	0
7	0.3844	0	0	0	0
8	0.1978	0.3305	0	0	0
9	0.0374	0.0625	0.3609	0	0
10	0.1360	0.0772	0	0	0
11	0	0	0	0	1.0000
12	0.1585	0.2045	0.1451	0	1.0000
13	0.0681	0.0878	0.0623	0	0.2567
14	0.0469	0.0266	0	0.1155	0
15	0.1201	0.0682	0	0.2957	0
16	0.2004	0.1137	0	0.4935	0
17	0.0801	0.1034	0.0734	0	0.3022
18	0.0118	0.0153	0.0108	0	0.0446
19	0.0141	0.0080	0	0.0348	0
20	0.0118	0.0067	0	0.0291	0

From Table 2.4, we can see that Gen 1 contributes most to the line 1 flow. For relieving line congestion, we choose to decrease the output of the most contributing generator and increase the output of the least contributing generator for the same amount. We simply choose a generator pair, for example, Gen 1 – Gen 4 pair. Let Gen 1 reduces its output by (1.1446-1.0-0.0849)/0.406=0.147 p.u., Gen 4 increases the output by 0.147 p.u. The new line 1 power flow result is 0.9782 p.u., which is very close to the scheduled 1 p.u..

If load management is available, the Load Contribution Factor can be calculated. Then appropriate amount of load management will be chosen. The generator re-dispatching and load management can be combined together to get an optimal solution for relieving congestion.

2.11.2 Transient Stability Control Scheme Case Study

Assume the following control means are available: all generators have fast valving (decrease up to 20% capacity), braking resistors (up to 50% capacity), line switching, TCSC (up to 50% compensation capacity of that line), SVC (up to 50MVA capacity), all buses have shunt reactors and capacitors (up to 50MVA capacity), load shedding. Simply use the classical machine model for the step-by-step (SBS) method and PEBS method.

Assume that at t=0s, a three-phase-to-ground-fault occurs at 95% of line 9-14. The critical clearing time (CCT) of step-by-step (SBS) method is 0.06s, and the CCT of PEBS method is 0.09s. There is a small difference between the SBS and PEBS methods due to numerical reason. When the fault is cleared at t=0.1s, we get the machine rotor angle curve given as below in Figure 2.6, where Gen 1's angle goes upward and all other generators' angles go downward. The transient energy margin is –0.042 by PEBS method.

All rotor angles in Figure 2.6 ~ 2.9 are in degrees. Total simulation time is 3s. The maximal angle difference is chosen as the angle stability criterion. If the maximal angle difference among all machines is bigger than 90^0 at t=3s, the system is unstable. Otherwise, the system is stable. In the following we give two control means, line switching and load shedding, which can stabilize the system.

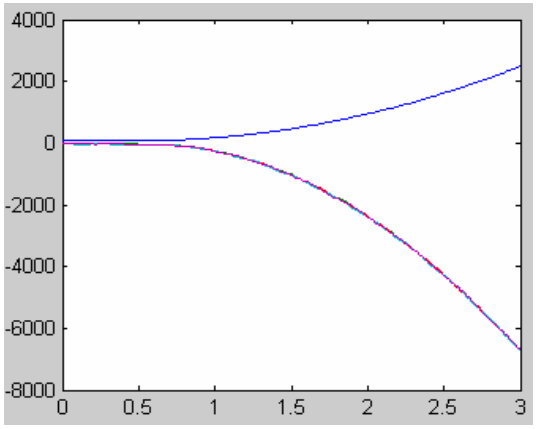

Figure 2.6 Machine angles when clear fault at t=0.1s

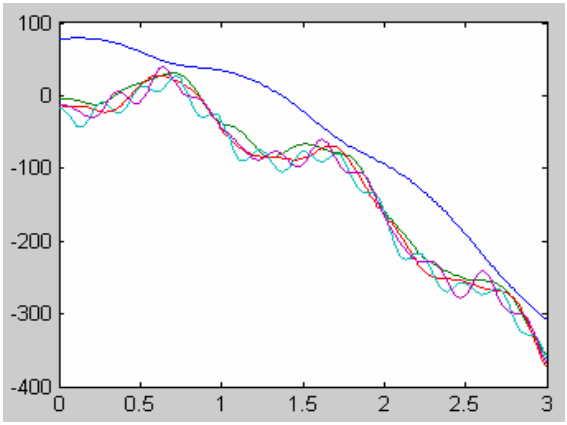

Figure 2.7 Angles when switching line 1-2 at t=0.11s

A. Stabilizing Switching

We get the new transient energy margin after switching additional single line as given in Table 2.5.

Table 2.5 New Transient Energy Margin after Stabilizing Switching

Line	1-2	7-9	4-7	4-9	5-6
Energy Margin	-0.007	-0.025	-0.027	-0.028	-0.033

We only list the top 5 lines, which contribute positively for stabilizing the system. Besides these 5 lines, the switching of line 2-3, 6-11, 13-14 also contributes positively for the stabilizing. Switching line 7-8 will result in islanding. The switching of other lines contributes negatively to stabilizing. The sensitivity analysis is not very accurate because of the first order approximation. Thus, we need to check with transient stability program. Take the example of line 1-2 switching, which contributes the most to stabilizing, as described in Figure 2.7. We can see that the energy margin after this switching is –0.007. That means the system is still unstable after this control. However, by the angle difference criterion in the time domain transient stability program, the system can be judged as stable.

B. Load Shedding

Assume the constant impedance model and the area load can be shed simultaneously with the same ratio. From the analytical sensitivity of the transient energy margin, we can get that the 24.5% load shedding is needed for the energy margin changing from negative to positive value. In fact, by the transient stability program, only 5.5% load shedding can make the system stable. Figure 2.8 is the rotor angle curve obtained by shedding 5.5% load. Figure 2.9 is the rotor angle curve obtained by shedding 24.5% load.

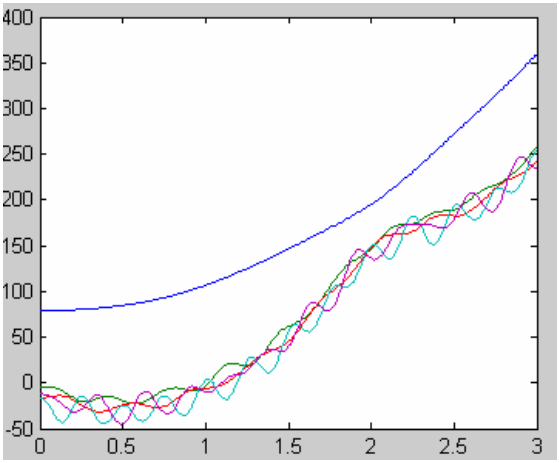

Figure 2.8 Machine angles when 5.5% load shedding at t=0.11s

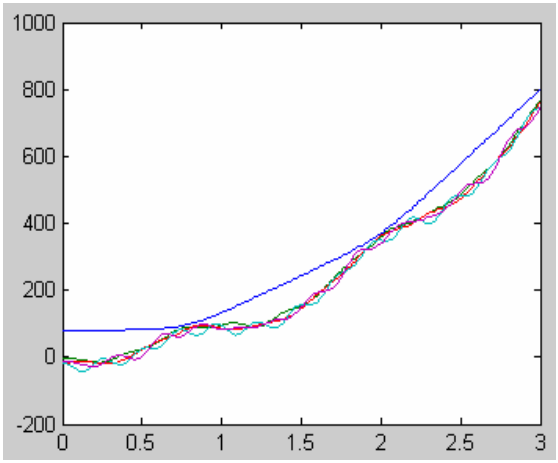

Figure 2.9 Machine angles when 24.5% load shedding at t=0.11s

2.12 Conclusions

The system-wide monitoring and control tool can perform routine and event-based security analysis, as well as steady state and transient stability control analysis. It uses the fast network contribution factor (NCF) method to get approximate steady state power flow results after network parameter(s) variance and static contingency. The approach is based on the network information and base flow condition. It uses the comprehensive vulnerability index (VI) and margin index (MI) to evaluate the vulnerability and security margin information of individual elements and whole power system. Thus the power system operation and contingency influence can be ranked by the combination of NCF, VI and MI methods. The steady state problems, i.e., branch overload or low voltage, can be solved by the steady state control scheme using NCF, GCF(generator contribution factor) and LCF(load contribution factor) methods. The transient stability control means are classified into two categories: admittance-based control (ABC) means and generator-input-based control (GIBC) means. The transient stability control can be implemented by using PEBS (potential energy boundary surface) method and analytical sensitivity of transient energy margin. Case studies of the steady state and transient stability control schemes for the modified IEEE 14-bus system show promising results of these two schemes. Dynamic relay analysis can be obtained during the transient stability simulation. The important and possible vulnerable distance relays can be found by the topology processing, static and dynamic relay analysis. Those relays will be chosen for careful monitoring by the local monitoring and control tool.

3. Local Monitoring and Control Tool

3.1 Introduction

The causes for large-scale blackouts are quite unique due to the complexity of power system operations. According to the historical data [27], relay misoperation is one of the contributing factors of 70 percent of the major disturbances in the United States. The major problem of conventional relays is that they make the decisions based on local measurements. In certain situations, the conclusion made by a local relay may not be suitable from a global standpoint. In addition, the relay hidden failures may be another factor to cause relay misoperations [28]. Inadequate local level diagnostic support is another factor that may contribute the blackouts. When disturbances occur, if the detailed local information cannot be delivered from the substations to the centralized system in an effective way, the system operator may not be able to make an informed decision and issue corrective controls on time.

One of the most important requirements to prevent system-wide disturbances at the substation level is to improve the performance of protection using the real-time analysis tools. This idea is consistent with some NERC recommendations, shown in Table I, which were formalized as a consequence of the final report about the Aug 14, 2003 blackout [12].

Table 3.1 Some NERC Recommendations to Prevent Cascading Events

21	*"Make more effective and wider use of system protection measures."*
22	*"Evaluate and adopt better real-time tools for operators and reliability coordinators."*
28	*"Require use of time-synchronized data recorders."*

The idea of wide area protection and emergency control is proposed to prevent the system-wide disturbances [29]. The wide area protection and control uses system-wide information and selected substation information to counteract the propagation of major disturbances. Availability of advanced computer, communication and measurement technologies makes the analysis approaches developed at the local substation level very helpful for implementation of a wide area protection and control system.

Local monitoring and control tool aims at two goals:

(a) Improving real-time fault analysis by more "intelligent" fault analysis approaches. The Neural Network based Fault Detection and Classification (NNFDC) algorithm and Synchronized Sampling based Fault Location (SSFL) algorithm are combined as an advanced real-time fault analysis tool to provide fault information that is more reliable and accurate than provided by the traditional distance relays.

(b) Validating relay operations by event analysis tools. The event tree analysis (ETA) is an efficient tool for implementing contingency/response based analysis and it is used

for comparing actual relay operations with the expected ones. Corrective control actions are introduced if the relay operations are not as expected.

By using the proposed schemes, the system monitoring and control tool can obtain more useful fault analysis information from the substation level. Having this information, the system operators can respond to the disturbances more quickly and with greater chance to prevent or mitigate the propagation of those disturbances.

3.2 Neural Network Based Fault Detection and Classification (NNFDC)

A self-organized, fuzzy ART neural network based fault detection and classification algorithm has been developed and described in [30]. The structure of the Fuzzy ART neural network algorithm and its application are shown in Figure 3.1. The two grey blocks are the key components of the algorithm: ART neural network training and Fuzzy K-NN classification. The theoretical background of these two approaches can be found in [31,32]. By using those techniques, the fault detection and classification becomes a pattern recognition approach instead of phasor computation and comparison. Voltage and current signals from the local measurement are formed as patterns by certain data processing method [33]. Thousands of such patterns obtained from power system simulation or substation database of field recordings are used to train the neural network offline and then the pattern prototypes are used to analyze faults on-line by using the Fuzzy K-NN classifier. The ART neural network is also capable for on-line training to update the pattern prototypes.

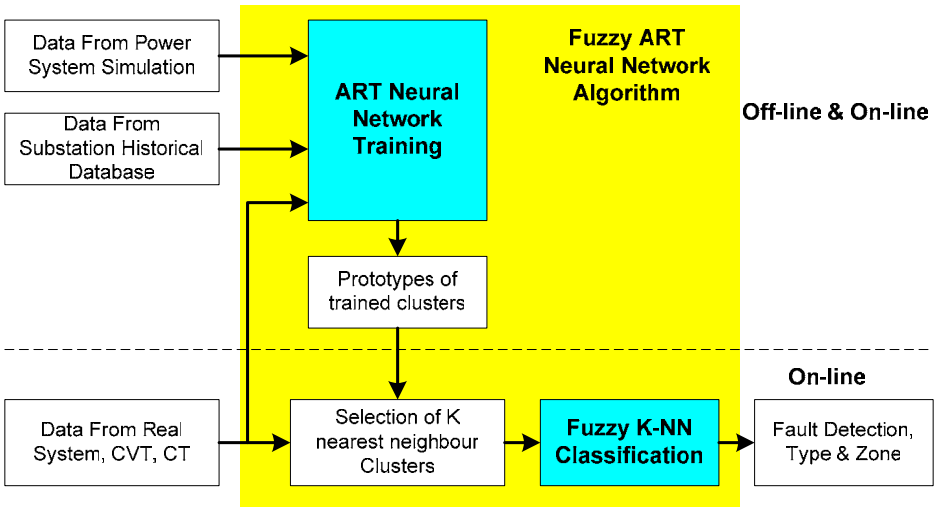

Figure 3.1 Fuzzy ART neural network algorithm

The aim of the algorithm is to allocate the training patterns into homogeneous clusters by some grouping technique. Then the clusters are assigned to the classes, which are our expected fault events in power system, such as “ABG_zone_I”, etc. The process is demonstrated using a 2-D demo shown in Figure 3.2. The ART neural network based on

unsupervised-supervised learning is very effective when trained with large data sets due to its special clustering techniques. The number of clusters is increased and their positions are updated automatically during the learning, and there is no need to define them in advance. By continuous iteration of unsupervised and supervised learning, a set of clusters that represent the desired outputs are obtained.

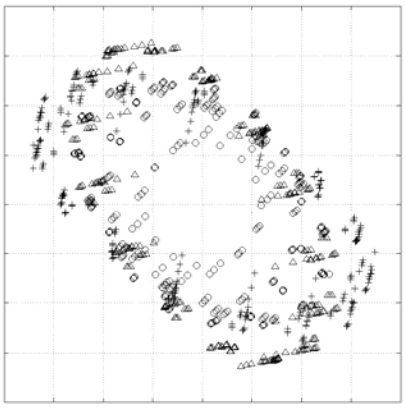

(a) The raw training patterns from three classes

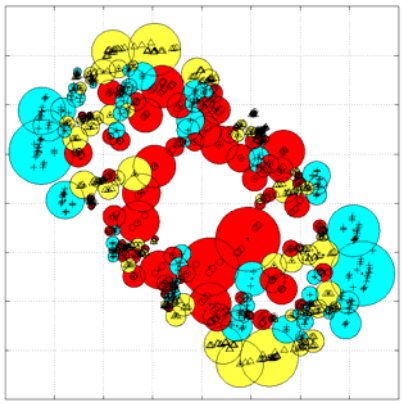

(b) The patterns are allocated to the clusters after a training process

Figure 3.2 A 2-D demo of ART neural network training

Using the prototypes of trained clusters, Fuzzy K-nearest neighborhood classifier can realize on-line analysis of unknown patterns for fault detection and classification [30]. The Fuzzy K-NN classifier takes into account both the effect of weighted distances and the size of neighboring clusters for distinguishing new patterns. It is proved that it has better performance than a common K-nearest neighborhood classifier [30].

The advantage of neural network based fault detection algorithm is that the neural network can form its “knowledge” by learning as many fault scenarios as it is presented and does not need to make compromise when determining settings as we do today when applying conventional distance relay schemes. The unsupervised/supervised training based fuzzy ART neural network algorithm has demonstrated additional benefits when dealing with large data set and algorithm convergence [30].

3.3 Synchronized Sampling Based Fault Location (SSFL)

Fault location techniques are used to precisely determine location of a fault on a transmission line. They are very important because the fault location can confirm whether a fault has indeed occurred on the line. If used on-line, it can also serve as a relay verification tool for a back-up fault detection algorithm. When the fault is precisely located, one should know which breakers are responsible to clear that fault, and unnecessary trips that could spread an outage should be avoided. Both the dependability

and security of protection system operation will be improved by incorporating a precise fault location function.

Synchronized sampling based fault location algorithm uses raw samples of voltage and current data synchronously taken from two ends of the transmission line [34]. This can be achieved using Global Positioning Satellite (GPS) receivers, which generate the time reference for data acquisition equipment.

The algorithm is derived by solving the classic transmission line differential equations [34,35]. Short line algorithm and long line algorithm are derived using lumped RL line parameters and distributed RLC line parameters respectively. The principle of this algorithm is demonstrated with the transmission line shown in Figure 3.3. The voltage and current at the faulted point can be represented by both sending end data and receiving end data using linear relationship because the homogenous parameter line is separated by the fault point. If there is no fault on the line, the fault location cannot be found because there are multiple solutions in that case. Different algorithms use different techniques to find the fault point [36].

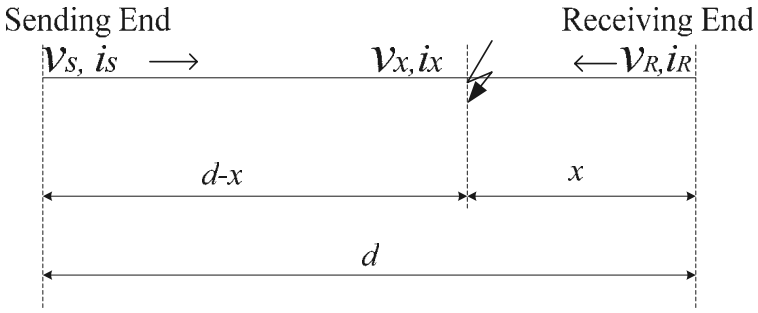

Figure 3.3 A faulted transmission line

For short line, which is usually shorter than 50 miles, the fault location can be calculated directly using minimum square estimate method, as follows [36]:

$$x = \frac{-\sum_{m=a,b,c}\sum_{k=1}^{N} A_m(k)B_m(k)}{\sum_{m=a,b,c}\sum_{k=1}^{N} B_m^2(k)} \tag{3.1}$$

where

$$A_m(k) = v_{mS}(k) - v_{mR}(k) - d\sum_{p=a,b,c}\left[\left(r_{mp} + \frac{l_{mp}}{\Delta t}\right)i_{pS}(k) - \frac{l_{mp}}{\Delta t}i_{pS}(k-1)\right] \qquad m = a,b,c \tag{3.2}$$

$$B_m(k) = \sum_{p=a,b,c}\left\{\left(r_{mp} + \frac{l_{mp}}{\Delta t}\right)\left[i_{pS}(k) + i_{pR}(k)\right] - \frac{l_{mp}}{\Delta t}\left[i_{pS}(k-1) + i_{pR}(k-1)\right]\right\} \qquad m = a,b,c \tag{3.3}$$

where k is the sample point, Δt is sample period, subscripts S, R stand for the values from sending end and receiving end of the line.

For long transmission line model, we can only build the voltage and current profiles along the line using revised Bergeron's equation [35]:

$$v_{j,k} = \frac{1}{2}\left[v_{j-1,k-1} + v_{j-1,k+1}\right] + \frac{Z_c}{2}\left[i_{j-1,k-1} + i_{j-1,k+1}\right] - \frac{R\Lambda x}{4}\left[i_{j-1,k-1} + i_{j-1,k+1}\right] - \frac{R\Delta x}{2} i_{j,k} \tag{3.4}$$

$$i_{j,k} = \frac{1}{2Z_c}\left[v_{j-1,k-1} - v_{j-1,k+1}\right] + \frac{1}{2}\left[i_{j-1,k-1} + i_{j-1,k+1}\right] + \frac{R\Lambda x}{4Z_c}\left[i_{j-1,k+1} - i_{j-1,k-1}\right] \tag{3.5}$$

Where $\Delta x = \Delta t / \sqrt{lc}$ is the distance that the wave travels with a sampling period Δt ; $Z_c = \sqrt{l/c}$ is the surge impedance. Subscript "j" is the position of the discretized point of the line and "k" is the sample point.

The final location is obtained by an indirect method, as shown in Figure 3.4.

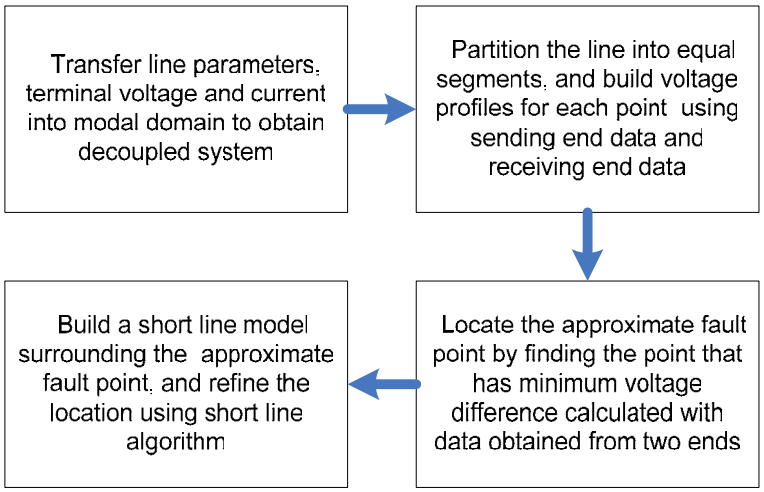

Figure 3.4 Steps for long line fault location algorithm

The accuracy of both algorithms is dependent on accuracy of data sampling synchronization, sampling rate and correctness of line model parameters.

Compared to the fault location algorithms that use one end data, SSFL makes no assumptions about fault condition and system operating state. Therefore it is less affected by those factors. Compared to the traditional impedance based algorithms involving phasor calculation, SSFL uses raw data from time domain. Therefore it keeps the useful information in the waveform to locate the fault precisely.

3.4 Advanced Fault Analysis Tool Based on NNFDC and SSFL

The development and testing of NNFDC and SSFL individually have demonstrated their advantages over traditional line protection algorithms. The combination of these two

algorithms is even more attractive. Developed by two different principles and based on different implementations, the two algorithms complement each other providing a complete and accurate reference about fault detection, classification and location. The two algorithms are optimized first to be more feasible in practical applications. The integration scheme is then demonstrated.

3.4.1 Optimization of NNFDC

The transmission line fault has great randomness because of the different combination of fault parameters, system conditions and system-wide disturbances. The argument that neural network based algorithm has better performance than conventional distance relay is based on an assumption that the neural network has broader view of system contingencies after a comprehensive learning process. The neural network based algorithms face the issue of dealing with the large set of training data. Although the ART neural network does convergence faster than MLP neural networks, it is still necessary to find an efficient way to train the neurons.

A scheme using three Fuzzy ART neural networks is proposed to deal with several application issues [9]. The proposed scheme is demonstrated to be more efficient in neural network training and more accurate in fault analysis than the previous method using only one neural network to take over all the tasks.

In the proposed strategy, neural network #1 (NN1) serves as a starting function to initially detect the fault events within a predefined area, which is usually larger than the far-most protection zones looking from both ends of a transmission line. There are only two outputs from NN1. “Fault” means a fault occurred within predefined area and “normal” means no fault occurred in that area. NN1 takes into account as much as possible fault events that may affect the desired detection. The training process is not significantly involved since there are only two outputs.

Neural network #2 (NN2) is used to refine the classification of the “fault” events detected by NN1. While the fault events for training NN1 may be sparsely distributed in the power system, the ones for training NN2 will have more focus on the desired zones and zone margins to achieve more accurate conclusions. The output of NN2, according to the classification objective, describes specific event types (normal, AB/ABG, BC/BCG, CA/CAG, ABC/ABCG, AG, BG, CG), or combines the zone information (Zone I, Zone II, Zone III or reverse Zone).

Neural network #3 (NN3) separates two-phase faults from two-phase-ground faults. This issue was not solved before because their feature difference is not prominent enough by using three phase voltage and current as training patterns. The major difference in these two types of faults is the magnitude of neutral voltage and current during the fault. Therefore the training patterns for NN3 are derived from the time domain signal $3u_0 = (u_a + u_b + u_c)$ and $3i_0 = (i_a + i_b + i_c)$. Two outputs of NN3 indicate whether the fault involves ground.

The advantage of coordinating the three neural networks is the distribution of large input set into different neural networks to reduce the burden of training and testing. NN1 has large number of inputs but few outputs, providing an initial crude conclusion where the

faults are located. NN2 takes more patterns from limited areas to refine classification. NN3 uses different training features to detect whether the fault involves ground.

3.4.2 Optimization of SSFL

The original version of SSFL is an independent algorithm with no fault information known or assumed. If fault type is known in advance, SSFL can be further optimized to achieve a better accuracy and reduced computation time.

For short line algorithm, if fault type is known, there is no need to calculate the healthy phases in equations (3.2) and (3.3) since there is no unique location *x* that can be found in equation (3.1) in healthy phases. The calculation is redundant and the error may be introduced in such cases.

For long line algorithm, when the phase values are transferred to the modal domain, not all fault types can be located correctly using a single mode. For example, if we use Clarke transformation matrix for mode decomposition, the ability to locate the different fault types using different modes is shown in Table 3.2. Obviously, if fault type is not known, we have to select at least two modes to obtain the correct location for all types. When the fault type is known, we can select only one mode to do the calculation. Therefore, the fault type classified by NNFDC is very helpful for SSFL to improve the fault location calculation. Another issue is that the original algorithm requires the modal values be transferred back to the phase values when building a short line model to refine the location. That process is pretty complex and time-consuming.

Table 3.2 Capability of Different Mode to Locate the Different Fault Type

	AG	BG	CG	AB	BC	CA	ABG	BCG	CAG	ABC/ ABCG
Mode 0	Y	Y	Y	N	N	N	Y	Y	Y	N
Mode 1	Y	Y	Y	Y	N	Y	Y	Y	Y	Y
Mode 2	N	Y	Y	Y	Y	Y	Y	Y	Y	Y

Through a variety of performance studies, the following method that will have better performance and efficiency is found:

- Fault type is not known: Mode 1 and Mode 2 are selected for the calculation.
- Fault type is known: Mode 0 is selected to locate ground faults and Mode 2 is selected for the aerial faults.

Either of the two approaches does not require the data be transferred back to phase domain when refining the fault location using short line algorithm.

3.4.3 Integration of NNFDC and SSFL

The entire scheme for fault detection, classification and location using NNFDC and SSFL is shown in Figure 3.5. The figure reflects the optimization of both algorithms mentioned

above. Such structure is based on the analysis of the advantages and shortcomings of the two algorithms. For NNFDC, it only takes local data with sampling rate as used in distance relays. The scheme can quickly detect the fault and conclude the fault type, and can even send a trip or block command if necessary.

The NNFDC can only conclude the fault zone crudely due to its local view. SSFL can locate the fault more precisely and confirm the fault detection obtained from NNFDC. However, there is a time delay due to transmitting synchronized data from two ends of a transmission line. Concerning this delay, the fault type information will be already available from NNFDC when SSFL implements the calculation. This information can be used by SSFL to improve the fault location calculation. The integrated algorithm requires only one cycle or less of time domain voltage and current data and can be used for on-line monitoring and actual protection system as long as the measurements and communication requirements are satisfied.

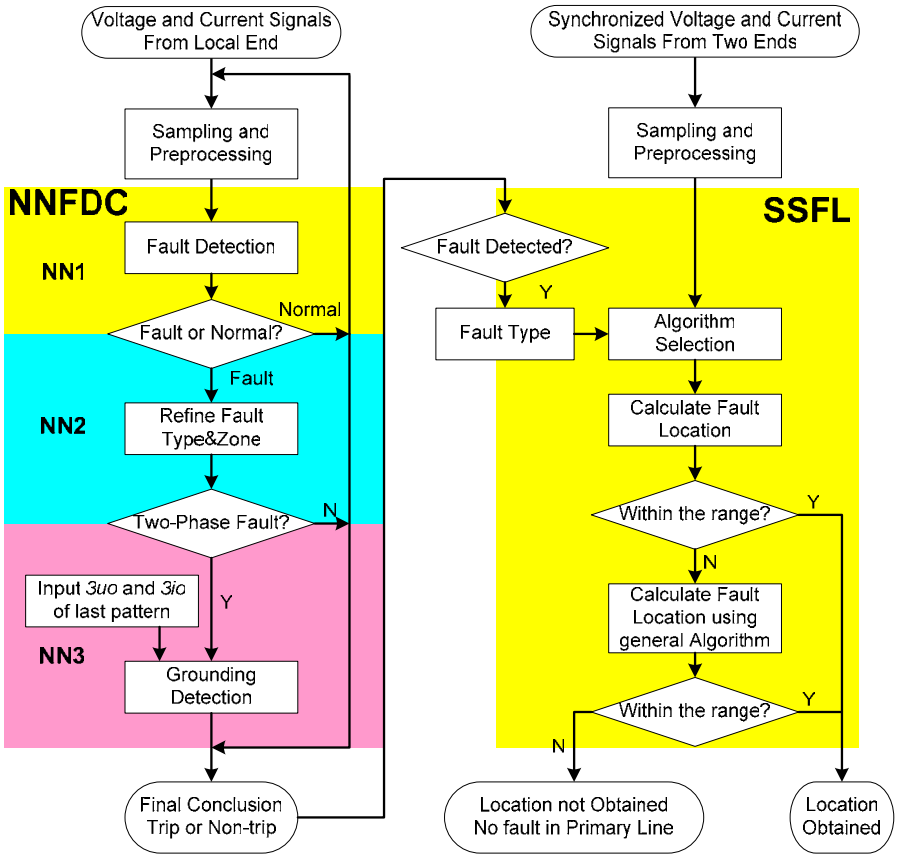

Figure 3.5 The scheme using combination of two algorithms

3.4.4 Field Configuration of Proposed Fault Analysis Scheme

A possible field configuration of proposed fault analysis scheme is shown in Figure 3.6. Ideally, the fault analysis tool will be installed at each EHV substation. NNFDC does not

require extra equipment. The input data can be sampled by regular A/D conversion, which is commonly used in distance relays. For SSFL, it requires synchronized data from both ends and high sampling rate usually in the order of 10-100 kHz is preferred. High frequency sampling unit, such as digital fault recorder (DFR), is required for high accuracy fault location. The synchronized data should be transmitted between the transmission line ends using standard data format such as IEEE standard 1344–1995 [33], or COMTRADE [35]. The synchronized data of voltage and current samples do not need to be converted to a phasor. Only the raw data samples in time domain are required. With fast fiber-optic and digital-communication systems, high speed data transfer can be achieved and only a small time delay will be introduced in transmitting the data.

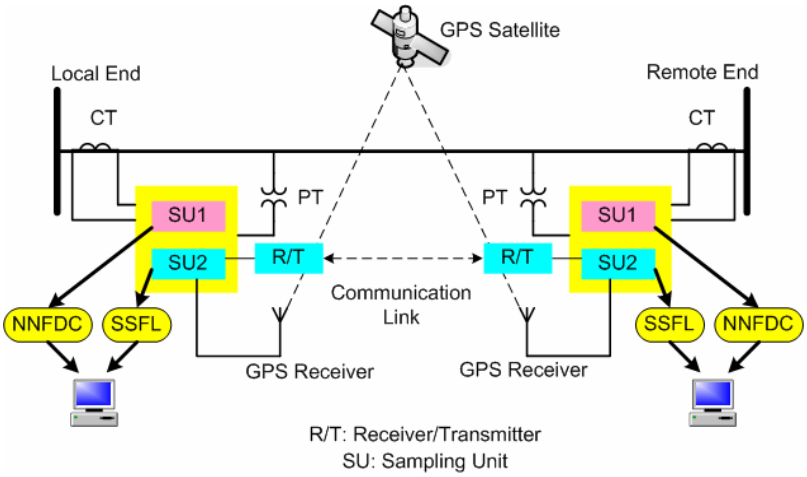

Figure 3.6 Configuration of proposed scheme

3.5 Monitoring Relay Operations by Event Tree Analysis (ETA)

Two main causes of the August 14, 2003 blackout were [12]: i) Inadequate situational awareness, and ii) Inadequate diagnostic support. When disturbances occur in the system, the system operator usually cannot get the detailed information about what is going on in the substations in a short time. Having the proposed real-time fault analysis tool at the substation level, we can create a relay monitoring process to verify the event sequence after the disturbance happens. Event tree analysis (ETA) is a commonly used event/response technique in industry for identifying the consequences following an occurrence of the initial event [39,40]. It was first applied in the risk assessments for the nuclear industry but is now utilized by a lot of other industries such as chemical processing, gas production and transportation.

The Event Tree Analysis takes the structure of a forward (bottom-up) symbolic logic modeling technique. This technique explores system responses to an initial “challenge” and enables assessment of the probability of an unfavorable or favorable outcome [40].

Figure 3.7 shows a very simple event tree for a gas leak protection system. The initiating event is the gas leak from an offshore platform. The branches then consider the success

(S) and failure (F) of the gas protection system. The outcome determined by the end-point of each event tree branch identifies a different consequence following the initiating event. The probability of each outcome can be evaluated if we know the likelihood of each node passing along the branches.

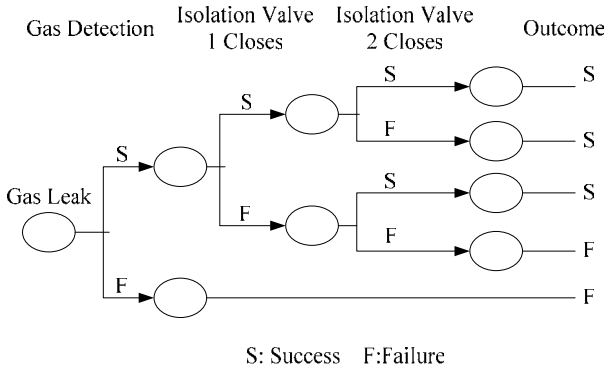

Figure 3.7 A sample event tree for gas leak alarming system

There are not very many applications for the event tree analysis in the power systems so far. Reference [41] introduced a dynamic decision event tree (DDET) method to prevent system blackouts. The idea is very good but because of the randomness of the power system events, it is very difficult to predict all the initial events and their unfolding contingencies. Therefore, it may still be difficult to implement the idea in a real system.

To utilize the event tree analysis more efficiently, the initial event and the following events must be foreseen. By doing this, all of the possible events and actions can be covered by the event tree analysis. Considering the single relay system, consisting of a distance relay, its associated circuit breaker and communication equipment, the possible contingencies are finite and can be foreseen. In spite of randomness, it is still possible to predict all the events for each relay system if its configuration is known. Therefore, the event tree analysis method can be used rather efficiently in monitoring the relay system operations.

For a distance relay system at one end, at least three event trees need to be built to respond to the possible disturbance based on three types of initial events: (1) No fault detected in either primary zone or backup zones, (2) Fault detected in the primary zone, and (3) Fault detected in backup zones. Figure 3.8 - 3.10 demonstrate the event trees that match the three cases. The explanation of each node in the event trees and its corresponding reference actions are given in the associated tables.

The event trees we built have been extended from the original format. In those figures, the nodes stand for the events or actions, where the white nodes represent correct actions and the black nodes represent incorrect actions. Following a set of events or actions from the root node (initial event), the event tree reaches an outcome that indicates whether the overall action is appropriate or not for a corresponding disturbance. If the event sequence is heading to or already reached a “black” node, a corrective action must be taken.

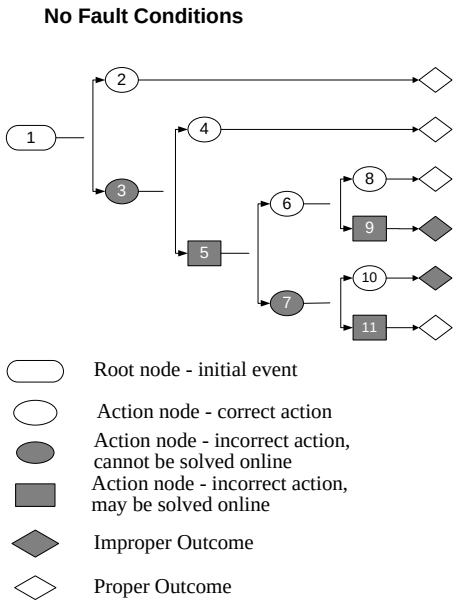

(a) Event Tree #1

Node	Scenarios	Reference Action
1	No fault in preset zones	Keep monitoring
2	Relay does not detect a fault	Stand by
3	Relay detects a fault and initiates a trip signal	Check the defects in relay algorithm and settings
4	Trip signal blocked by the other device in the system	
5	Trip signal failed to be blocked	Check communication channel Send blocking Signal if necessary
6	Circuit breaker opened by a trip signal	
7	Circuit breaker fails to open	Check the breaker circuit.
8	Autoreclosing succeeds to restore the line	
9	Autoreclosing fails to restore the line	Send reclosing signal to the breaker
10	Breaker failure protection trips all the breakers at the substation	
11	No Breaker failure protection or it doesn't work	Check the circuit of the breaker failure protection.

(b) Node explanation and reference corrective actions

Figure 3.8 Event tree #1 for no fault condition

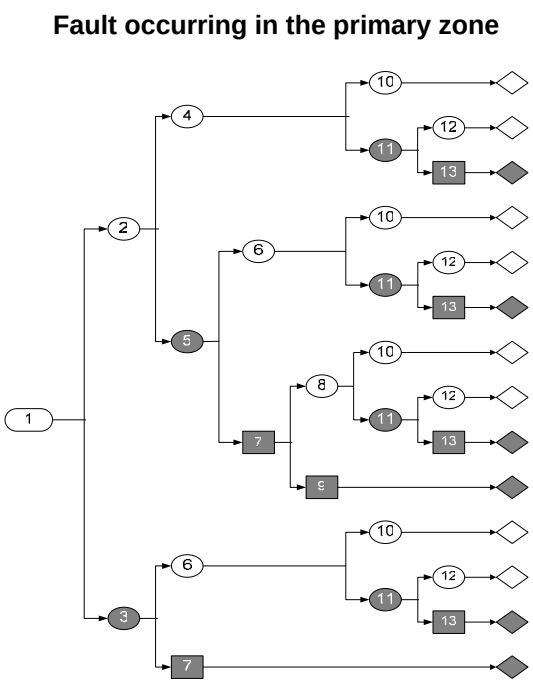

(a) Event Tree #2

Node	Scenarios	Reference Action.
1	Fault occurs in a primary zone.	
2	Relay detects the fault	
3	Relay does not detect the fault	Check defects in relay algorithm and settings
4	Relay sees the fault in a correct zone	
5	Relay sees the fault in an incorrect zone	Check defects in relay algorithm and settings
6	Transfer trip signal is received	
7	Transfer trip signal is not received	Check communication channel Send Trip Signal if necessary
8	Relay trips the breaker	
9	Relay does not trip the breaker; Fault is cleared by other breakers	Try to open the breaker associated with this relay and correct other redundant trips
10	Circuit breaker opened by a trip signal	
11	Circuit breaker fails to open	Check the breaker circuit
12	Breaker failure protection trips all the breakers at the substation	
13	No breaker failure protection or it does not work	Check the circuit of the breaker failure protection

(b) Node explanation and reference corrective actions

Figure 3.9 Event tree #2 for fault occurring in primary zone

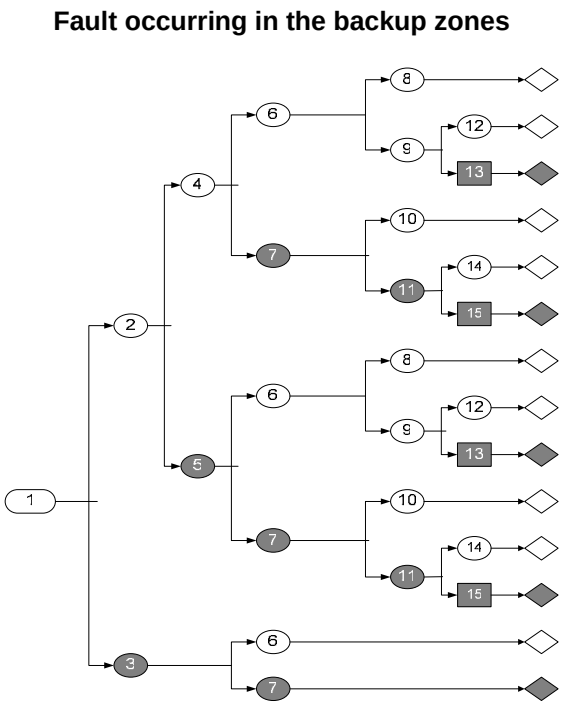

(a) Event Tree #3

Node	Scenarios	Reference Action.
1	Fault occurs in backup zone	
2	Relay detects the fault	
3	Relay does not detect the fault	Check defects in relay algorithm and settings
4	Relay sees the fault in a correct zone	
5	Relay sees the fault in a incorrect zone	Check defects in relay algorithm and settings
6	Other relays clear the fault successfully	
7	Other relays did not clear the fault successfully	
8	Back-up relay is reset or blocked	
9	Back-up relay is not reset or blocked	
10	Back-up relay trips the breaker	
11	Circuit breaker fails to open	Check the breaker circuit.
12	No unnecessary trips	
13	Unnecessary trip occurs	Try to restore the unnecessarily tripped lines
14	Breaker failure protection trips all the breakers at the substation	
15	No breaker failure protection or it does not work	Check the circuit of the breaker failure protection.

(b) Node explanation and reference corrective actions

Figure 3.10 Event tree for fault occurring in backup zone

3.6 On-line Application of Fault Analysis and Relay Monitoring Tool

3.6.1 Setup of the Fault Analysis Tool and Relay Monitoring Tool

Before the above techniques (fault analysis tool based on NNFDC and SSFL, and relay monitoring tool based on ETA) are used for on-line analysis, the analysis tool needs to be installed for each distance relay system at the substation.

For NNFDC, the neural networks need to be trained offline first by a variety of scenarios covering the different combinations of fault parameters, including fault type, location, resistance and inception angle. The training process should also take into account the system-wide disturbances, especially the fault and switching events in the surrounding lines. The input for training can be the waveforms obtained by power system simulation or combined with the substation field recorded data. The detailed training process is described in [9,30].

For SSFL, the important issue is finding the appropriate line parameters for each transmission line. For the short transmission line, usually shorter than 50 miles, the lumped line parameters can be used. For long transmission lines, the distributed line parameters should be used because the capacitance of the line cannot be neglected.

For ETA, the event trees for each distance relay system should be built in advance. The

distance relay system usually consists of the distance relay, circuit breaker, DC battery, communication equipment and other associated components. Taking into account the different configuration of each substation, the event trees may not be the same at each location. For each distance relay, the event trees should be able to explore all the possible responses of the relay system to the disturbances. After the event trees at the local level are built, they should be stored at the system level as an event tree database. A possible solution is shown in Figure 3.11. When a suspect disturbance is detected and analyzed at the local level, the local substations will send the event sequence reports to the system operator, who can extract the corresponding event trees and can have a graphic view of what was going on during the disturbance.

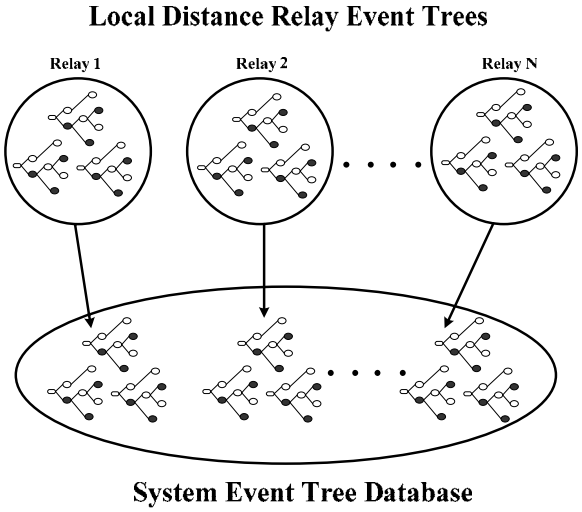

Figure 3.11 A possible local and system event tree coordination scheme

3.6.2 Implementation of On-line Analysis and Monitoring

The real-time fault analysis tool and relay monitoring tool are formed as the local monitoring and control tool to monitor system disturbances and the relay operations in substations. The structure of the local tool is shown in Figure 3.12. The real-time fault analysis could be a continuous process. When there is a suspect disturbance detected, event tree analysis process will be triggered, as shown in Figure 3.12.

When a suspect disturbance occurs, the first step is to determine which event tree should be applied through the real-time fault analysis. By monitoring the relay output signals and breaker status, we can then check the corresponding event tree to see if the actual relay operations are heading to the expected outcome. If not, the operation can be corrected before or after it is effective. The information about the local activities will be sent to the system control center and neighboring substations to further confirm the analysis result. If necessary, the system operator will send further corrective control commands, such as load shedding or line switching.

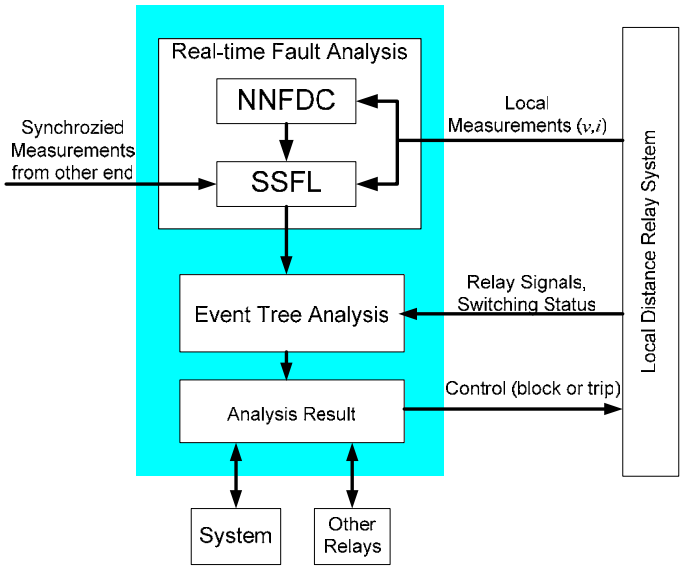

Figure 3.12 Block diagram of local monitoring and control tool

3.7 Power Swing and its Influences on Fault Analysis

3.7.1 Distance Relay Performance under Power Swing

The real power system is a dynamic system and the normal operation condition may be altered by certain disturbances caused by faults, load rejection, line switching, and loss of excitation. Power swing or even out-of-step may occur when mentioned disturbances happen [42]. Power swing and out-of-step condition is a typical phenomenon that can confuse the relay algorithms, making the relay trip on the no-fault conditions. If this happens in a stressed power system, the cascading blackout may probably be initialized in this case.

Distance relay for transmission line protection is designed to isolate the faults that occurred within the desired zone only. It is not supposed to trip the line during the power swing caused by the disturbances outside the protected line. Even for the out-of-step conditions, the preferred operation is to separate the system with an out-of-step tripping (OST) protection at pre-selected network locations and blocking other distance relays by out-of-step blocking (OSB) protection [42].

Power swing, either stable or unstable, may have impacts on distance relay judgment. The reason is discussed below.

An example of two machine system is shown in Figure 3.13. For steady state, assume the two sources have the terminal voltages as $E_{S0}\angle\delta_0$ and $E_{R0}\angle 0$ respectively, where the phase angle of the receiving end generator is always used as the angle reference. As for the two-machine system, the power swing appears to a relay as an oscillation of

magnitudes and the angles of two generators. At certain time during the power swing, assume the voltages are $E_S\angle\delta$ and $E_R\angle 0$.

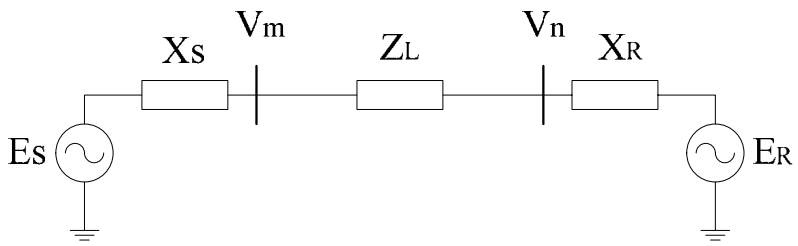

Figure 3.13 A two machine system

Then we have

$$\dot{I} = \frac{E_S\angle\delta - E_R\angle 0}{Z} \tag{3.6}$$

Where $Z = X_S + Z_L + X_R$. From Figure 3.13, we have

$$\dot{V}_m = E_S\angle\delta - jX_S \cdot \dot{I} \tag{3.7}$$

Therefore, the apparent impedance seen by the relay at bus *m* can be expressed as

$$Z_m = \frac{\dot{V}_m}{\dot{I}} = -jX_S + jZ\frac{E_S\angle\delta}{E\angle\delta - E_R} \tag{3.8}$$

The trajectory of Z_m with respect to E_S, E_R and δ can be found in [42]. When the angle difference δ becomes large enough, the trajectory of Z_m will float into the relay setting area and cause relay misoperation.

Now, let us extend the idea to regular multi-machine systems. Still look at Figure 3.13. Consider the line in the middle as one of the transmission lines in the system with the terminal voltages of $V_m\angle\theta_m$ and $V_n\angle\theta_n$. The other parts outside the line represent the rest of the system.

If there is no fault on the line, the impedance seen by relay at bus *m* is,

$$Z_c = \frac{\dot{V}_m}{\dot{I}_m} = \frac{\dot{V}_m}{(\dot{V}_m - \dot{V}_n)/Z_L} = Z_L\left(\frac{1}{1 - \left|\frac{V_n}{V_m}\right|\angle\theta_{nm}}\right) \tag{3.9}$$

According to (3.9), Z_c is only related to the magnitude ratio $(|V_n/V_m|)$ and angle difference $(\theta_{nm} = \theta_n - \theta_m)$ of the bus voltages at the two ends. When power swing occurs in the system, $V_m\angle\theta_m$ and $V_n\angle\theta_n$ will oscillate during that time. Assuming line impedance $Z_L = 1\angle 80°$, we

can draw the figure of Z_c trajectories in the R-X phase with respect to voltage magnitude ratios and angle differences, as shown in Figure 3.14.

This is very similar to the figures drawn in [42]. The conclusion is also similar as in the two-machine system. If the power swing causes θ_{nm} large enough, the impedance seen by relay will reach the zone settings and relay will misoperate.

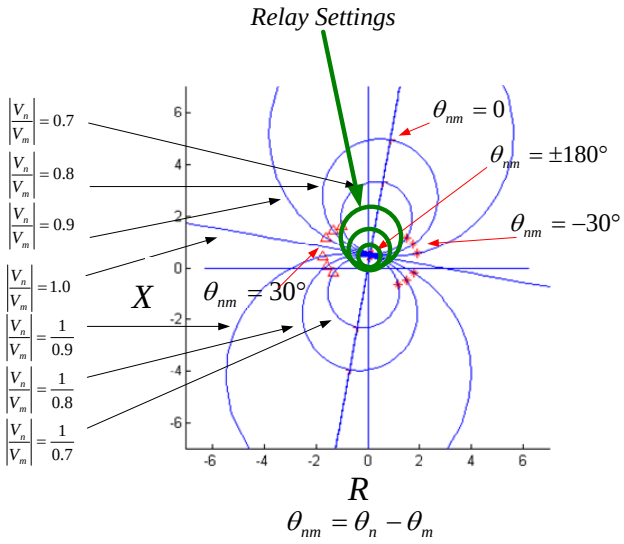

Figure 3.14 Z_c trajectory in the R-X phase

The analysis of the power swing effect can also be extended to other non-fault situations, such as overload and load encroachment, which may also cause relay misoperations. From the relay standing point, all of those non-fault situations will cause the changes of voltage magnitudes and the phase angles at the two ends of the transmission line. The difference is in the rate of change of those values. As long as the apparent impedance calculated by relay floats into the relay setting and satisfy the tripping condition, relay misoperation may happen. Since the power swing is a dynamic and relatively fast process, the evaluation of new fault analysis algorithm under power swing is typical of other no-fault contingencies.

3.7.2 NNFDC Under Power Swing

Most of neural network based transmission line protection algorithms use the time domain voltage and current samples as the pattern. It means they take the local measurements similar to those in distance relays. According to the analysis above, the power swing will cause the oscillation of the line terminal voltages. Hence, at some "snapshots" during the power swing, there may be low voltage and high current observed from the local stand point at one end of the transmission line. The patterns extracted at those snapshots may confuse the algorithm when considering other fault events. The reason is due to the lack of knowledge of power swing situations if the patterns from those situations are not trained by the neural network.

To avoid the misclassification, NNFDC needs to be improved to reduce the impact of power swing. The pattern prototypes need to be updated using more patterns generated during power swing. However, the power swing appears to be random in different situations. So it is not possible to train the algorithm with entire power swing process. An alternate method is proposed to solve this problem.

Whatever the power swing may look like, the phenomenon observed from transmission line is identical to periodical oscillation of voltage magnitudes and angle difference between the two ends as long as there is no fault on the line. Therefore, we can "imitate" the snapshot of the power swing by "adding" two ideal sources at both ends of the line of interest, as shown in Figure 3.15. By tuning the source magnitudes and phase angles, the "artificial" power swing patterns can be generated one at a time.

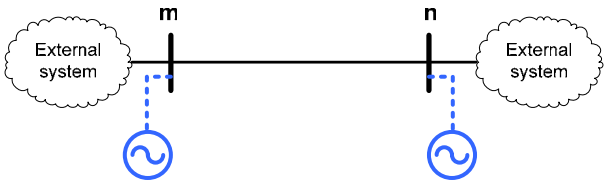

Figure 3.15 Scheme to generate "artificial" power swing patterns

3.7.3 SSFL Under Power Swing

The performance of SSFL algorithm during power swing relates to two situations. The theoretical analysis will be discussed here.

If there is no transmission line fault occurring during the power swing, the power swing may cause the false judgment of distance relays because the relay will see a low voltage and a high current during the swing. SSFL algorithm will avoid this misjudgment by its inherent characteristics. During the power swing, although the bus voltage and line current at two ends of line will oscillate from time to time, we still have the relation between the line currents seen from two ends $[i_{pS}(k)+i_{pR}(k)]\approx 0$. The reason is that the line parameters are still homogeneous along the entire line as long as there is no fault on it. Then, from (3.3) we have $B_m(k)\approx 0$. In this case, a reasonable fault location cannot be found using (3.1). Similarly, in the third step of the long line algorithm, as shown in Figure 3.4, if there is no fault on the line, the voltage difference computed using two ends data is almost the same along the entire line because the line parameters are homogenous. A prominent minimum point cannot be found. In this sense, the power swing will not affect the long line algorithm either.

If there is indeed a fault occurring during the power swing, the accuracy of SSFL in locating the fault needs to be evaluated. According to the algorithm derivation, there is no assumption about system conditions. Therefore, the influence of the power swing may be less than for other fault location algorithms. Reference [8] gives the detailed studies.

3.8 Algorithm Evaluation and Case Study

3.8.1 Performance Evaluation of New Fault Analysis Tool

This section presents comprehensive studies aimed at evaluating the performance of the integrated algorithm using NNFDC and SSFL. Three types of tests, with their objectives and methods, are listed in Table 3.3. The first two tests relate to the basic performance requirement of relays and the third one is a special case where the security of relay algorithms is tested under power swing and out-of-step conditions that can cause relay trip in no-fault situation [12,42]. Two complex power system models are selected to implement those tests, as shown in Figure 3.16 and Figure 3.17 respectively.

Table 3.3 Test Sets for Performance Evaluation

Test Set	System used	Objective and method
#1	**#1**	Test the overall dependability/security of the algorithm using randomly generated scenarios under different fault parameters and system conditions.
#2	**#2**	Test the selectivity of the algorithm using randomly generated system-wide disturbances.
#3	**#2**	Test the special security performance of the algorithm during power swing and out-of-step situation caused by initial disturbances

3.8.1.1 Power System Models

The two system models are implemented using Alternative Transient Program (ATP) [43]. MATLAB [44] is used to automatically generate a batch of simulation scenarios for testing the algorithms. Test #1 is performed using power system #1, which is a model of a real 345kV system section from CenterPoint Energy [45]. The system has a specific topology and actual line parameters. It is suitable to generate realistic fault scenarios in different system conditions. The STP-SKY line is the line of interest in this study. This is a long transmission line with distributed line parameters.

Test #2 and #3 are performed using power system #2, which is the WECC 9-bus system usually used in power flow studies and transient stability studies [46]. Unlike system #1, which is quite “strong” by having quite a few ideal sources, the 9-bus system represents a

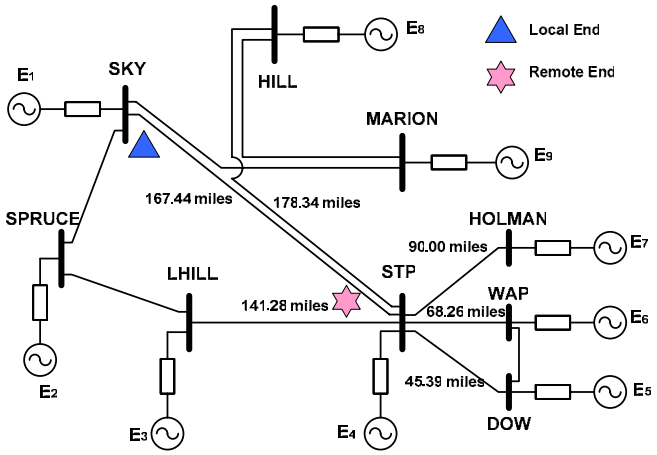

Figure 3.16 Power system #1: CenterPoint Energy STP-SKY model

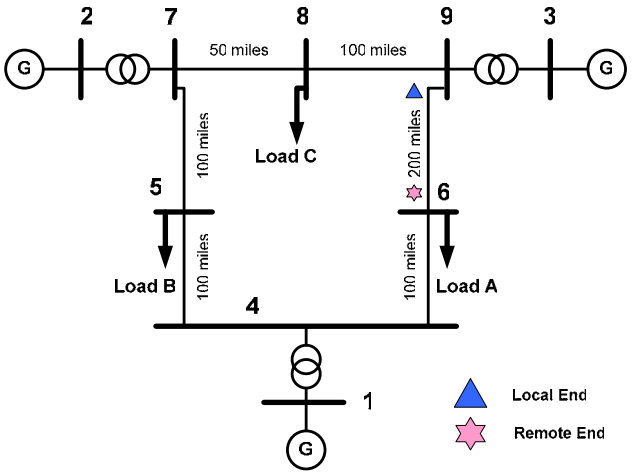

Figure 3.17 Power system #2: WECC 9-bus model

typical topology suitable to study the influence of system-wide disturbances. Since the generator data is also available in this system, a "dynamic" model is set up using the embedded synchronous machine component SM59 in ATP. The dynamic scenarios such as power swing and out-of-step condition can be simulated this way. The original lumped line parameters are modified to represent distributed parameters in our studies. The line of interested in this model is Line 9-6 with length of 200 miles, as shown in Figure 3.17.

For both systems, the proposed fault analysis algorithm is installed at the local transmission line ends and the synchronized data used in SSFL is transmitted from both remote ends.

3.8.1.2 Generation of Test Scenarios

For test #1, the disturbances involve only the events on SKY-STP line since the faults occurring in other areas have less influence on this line due to the strong in-feed configuration of the system. The integrated algorithm is used for classifying and locating the fault occurring on the SKY-STP line.

For NNFDC, since the measurement is taken from the local end only, at least two zones are needed to provide required security. In this test, zone I reaches 80% of the line SKY-STP looking from SKY bus. The rest of the line is covered by zone II. The training was implemented using the scenarios described in [30]. Only NN2 and NN3 are involved in this test since the events are only on the line SKY-STP. The number of training patterns is 3315 and 414 for NN2 and NN3 respectively.

Instead of scenarios which would only demonstrate the best performance of the algorithm, the randomly generated scenarios can demonstrate the overall performance and robustness of the proposed algorithm in all situations. The test scenarios in test #1 are generated using the method mentioned in [30]. The fault parameters are randomly selected from uniform distribution of: all fault types, fault distances (5%-95%), fault resistances (0Ω-30Ω), and fault inception angles ($0°$- $360°$). There are four types of

system conditions in this test and each has 500 random scenarios: a) Nominal system, b) Weak infeed (Disconnect E1 and E9), c) Phase Shift (E1 with phase shift -30°), and d) Frequency Shift (System frequency of 59Hz).

Test #2 evaluates selectivity of the proposed algorithm on Line 9-6 under system-wide events occurring in system #2. For NNFDC, we still use two-zone settings. Zone I reaches 80% of Line 9-6 and Zone II is up to 20% of Line 6-4. NN1 is used to decide whether a fault is occurring within Line 9-6 or Line 6-4. NN2 and NN3 are used to refine the classification of fault types and zones. The number of training patterns for NN1 is 9564, taken from fault scenarios involving each of the six lines.

The numbers of training patterns for NN2 and NN3 are 9240 and 1152 respectively, generated by different scenarios in Line 9-6 and Line 6-4 only. The test scenarios are generated randomly using the same fault parameter pool as in test #1. Each of the six lines in system #2 has 500 fault cases.

Power swing usually follows line switching, load change, or fault. In test #3, three kinds of typical scenarios outside Line 9-6 are selected to imitate the power swing phenomenon. Stable swing is simulated by line switching and line fault clearing that took place before the critical clearing time (CCT). Unstable swing (out-of-step) is simulated by the most severe three-phase fault cleared after CCT. An example of unstable power swing, which is caused by a three-phase fault on Line 4-5 and observed at the local end of Line 9-6, is shown in Figure 3.18.

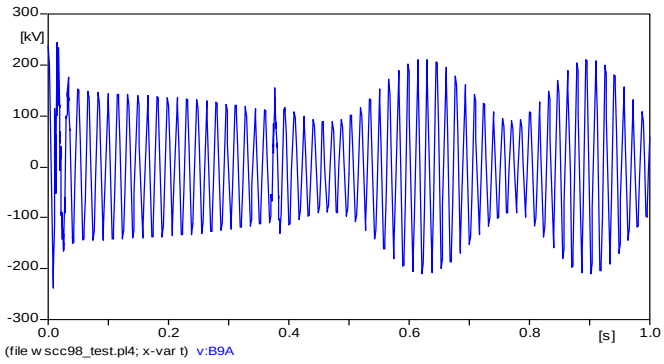

(a) Voltage profile of Phase A during power swing

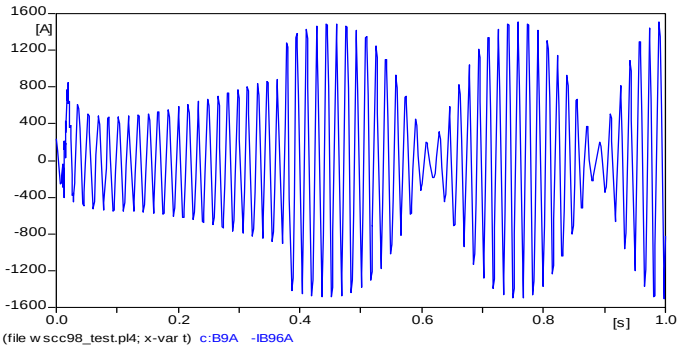

(b) Current profile of Phase A during power swing

Figure 3.18 An example power swing observed at Line 9-6 in power system #2

For all three tests, data sampling rate is 1.92 kHz for NNFDC and 100 kHz for SSFL. The data window for voltage and current samples is fixed to one cycle. In test #1 and #2, the data window is "static" and exactly taken from the post-fault value. In test #3, the data window is "dynamic" and slides throughout the entire power swing process.

3.8.1.3 Test Results and Discussions

The error of NNFDC in detecting and classifying the fault and the error of SSFL in locating the fault are reported for each test. The error of NNFDC is defined as

$$Error(\%) = \frac{(ne1 + ne2 + ne3)}{N} \times 100 \tag{3.10}$$

where *ne1*: Number of cases that NN1 misclassified "faults" within desired area as "normal".

ne2: Number of cases where NN2 misclassified either fault type or fault zone.

ne3: Number of cases that NN3 misclassifies two-phase-faults.

N: Total number of cases in the test set.

The error of SSFL is defined as:

$$Error(\%) = \frac{|Actual\,Location - ComputedLocation|}{Line\,Length} \times 100 \tag{3.11}$$

The results of test #1 are demonstrated in Figure 3.19. They indicate that for all four different system situations, NNFDC provides very good classification of fault type and SSFL provides very good accuracy of fault location. Those performances are almost transparent to the system conditions and have good consistency. Most of false type and zone classification cases in NNFDC are from test scenarios around the zone boundary, since the features of those fault scenarios are difficult to distinguish from just using the

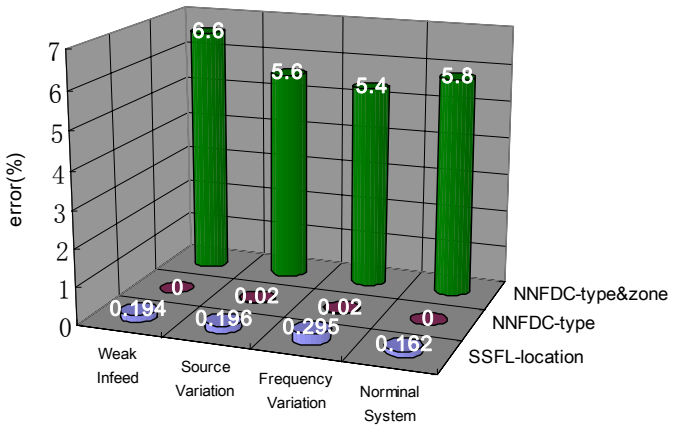

Figure 3.19 Classification and location error of test #1

local measurements. According to the results reported in [47], this kind of error is still much smaller compared with conventional distance relays.

The error of SSFL shown in Figure 3.19 is the average error of 500 cases in each system condition. The maximum error and minimum error in each case are listed in Table 3.4. The results indicate that SSFL is less affected by different system conditions.

Table 3.4 Location Error in Each System Condition

	Avg error (%)	**Max error (%)**	**Min error (%)**
Nominal system	0.1616	0.8516	0.0001
Weak infeed	0.1941	1.1128	0.0009
Source Variation	0.1959	1.1948	0.0003
Freq Variation	0.2953	1.0210	0.0001

The results of test #2 are shown in Figure 3.20. Fault type is still well classified by NNFDC. For all fault cases on six lines, the error of type and zone classification using NNFDC only appears on the primary line (9-6) and secondary line (6-4). Most of error cases are also from the scenarios around the zone boundaries. The results in the row "SSFL-zone" indicate that SSFL can successfully distinguish the faults occurring on the primary line from those on other lines. Fault location error on the primary line is a little bit higher than in test #1. The maximum and minimum errors are 2.8815% and 0.0016% respectively. The main reason is that for the same sampling rate, the discretized length (calculated by $\Delta x = \Delta t / \sqrt{lc}$) of Line 9-6 is larger than that of SKY-STP. The results in Figure 3.20 show that the integrated algorithm has good selectivity for the system-wide disturbances.

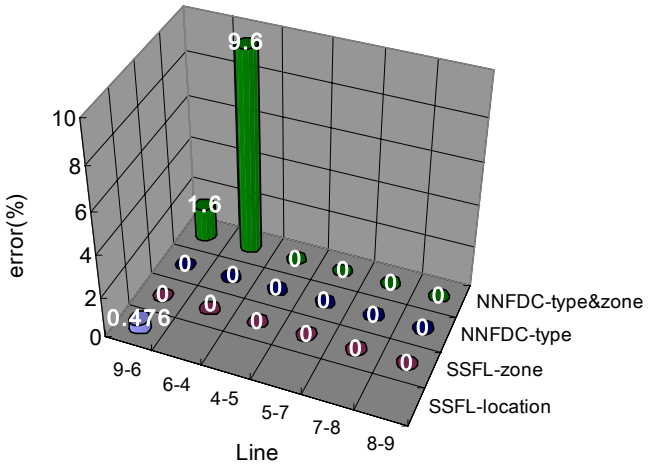

Figure 3.20 Classification and location error of test #2

For test #3, the desired behavior of the integrated algorithm is that it should not initiate a trip signal during the power swing. The reason is that power swing, whether stable or unstable, is not a fault within the line of interest. Therefore, the distance relay or other fault detection algorithm should not trip during the swing unless it receives the direction by out-of-step relays.

The results of test #3 listed in Table 3.5 demonstrate whether the two algorithms will trip for the power swing caused by different situations. During the entire power swing process, if either algorithm NNFDC or SSFL considers the swing as fault at three snapshots in a row, the false conclusion is then drawn by that algorithm. The result in Table 3.5 indicates that NNFDC avoided false trips on all stable swings but failed in some unstable swings. For SSFL, it is shown that it is not affected by power swing at all in any of the cases. The results justify the analysis in section 3.7.2 and 3.7.3.

Table 3.5 Test Result for Power Swing Simulation

Swing	Case	Line	NNFDC Correct?	SSFL Correct?
Stable	Line open	6-4	Yes	Yes
		9-8	Yes	Yes
		4-5	Yes	Yes
		5-7	Yes	Yes
		7-8	Yes	Yes
	Line fault (Clearing time <CCT)	4-5	Yes	Yes
		5-7	Yes	Yes
		7-8	Yes	Yes
Unstable	Line fault (Clearing time >CCT)	4-5	No	Yes
		5-7	No	Yes
		7-8	Yes	Yes

The following improvement is used for enhancing NNFDC under power swing conditions. Using the "artificial" method mentioned in section 3.7.2, NN1 is retrained by another 14400 patterns because NN1's main role is to differentiate power swings from faults. Applying the updated neural networks to test the scenarios in test #3, NNFDC did not misclassify the unstable swing as a fault this time.

3.8.2 Case Study for Monitoring Relay Operations

This section gives an example that how to use event tree analysis for relay monitoring. In order to monitor relay operation, traditional distance relay algorithm needs to be modeled in MATLAB as well. Traditional distance relay algorithm can be found in a lot of references, such as [48]. Using the computed phasors for three-phase voltages and currents, the apparent impedance of relay is estimated for each of the possible phase-to-phase (AB, BC, CA) and phase-to-ground fault types (AG, BG, CG). The impedances are

then compared to the *mho* and *quadrilateral* characteristics [49], as shown in Figure 3.21. Selection of *mho* or *quadrilateral* characteristic depends on value of zero sequence current. The existence of zero sequence current indicates ground fault and *quadrilateral* characteristic should be used, otherwise the fault does not involve ground and *mho* characteristic should be used. When the operating characteristic is chosen, the impedance is examined against all three sets of individual settings. The type and location of an actual fault is concluded by checking where the impedances fall within the zone settings. The timers of the zone settings are set as fixed values here.

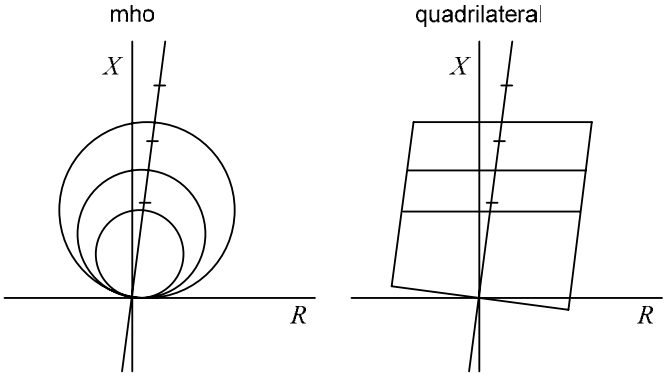

Figure 3.21 *mho* and *quadrilateral* characteristics

In order to demonstrate the overall process of the proposed event analysis method, an example based on the 9-bus system is shown in Figure 3.17. In the 9-bus system, assume there is a three-phase fault occurred at middle of line 4-5. Assume that for some reason, the trip signal is delayed and the circuit breakers at line 4-5 have opened very close to its critical clearing time (CCT). After the fault is cleared, the system experienced a power swing. As shown in Figure 3.22, the voltage and current for line 9-6 at bus 9 have the profile with an oscillation.

At a certain time, low voltage and high current are observed by this relay. The impedance calculated by this relay will float into the relay setting areas, as shown in Figure 3.23. The relay will detect the event as the Zone 3 fault. If the timer of Zone 3 expires, the relay will trip line 9-6. That will further worsen system stability. If such a scenario happens in a large system, a probable blackout may be initialized.

For this scenario, the conclusions of both NNFDC and SSFL indicate that there is no fault either in the primary zone or backup zones. This will send a signal to relay to block the backup protection. In this case, the event tree shown in Figure 3.8 should be selected to monitor the relay.

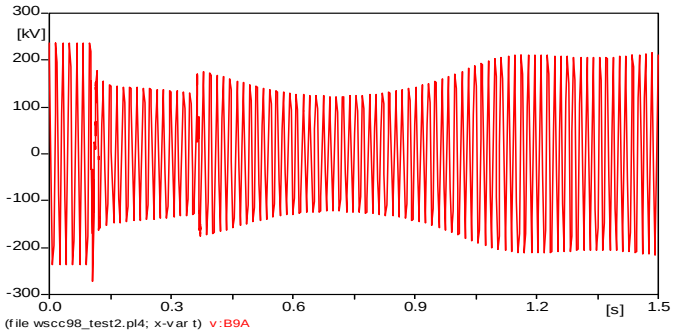

(a) Phase A voltage at bus 9 during the power swing

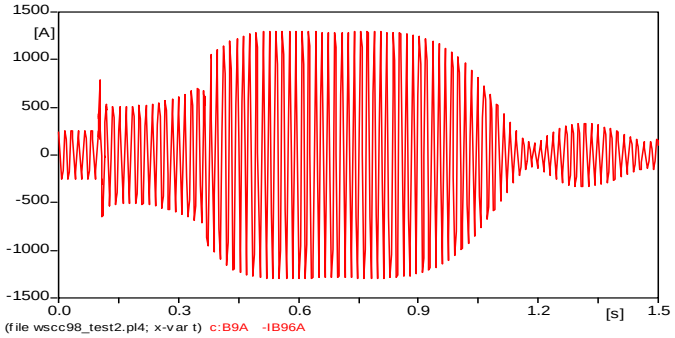

(b) Phase A current in line 9-6 during the power swing

Figure 3.22 Oscillation of voltage and current at bus 9 and line 9-6

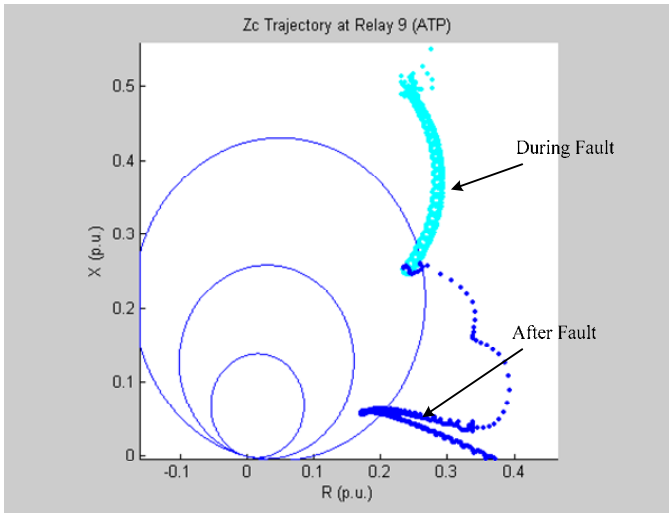

Figure 3.23 Trajectory of computed impedance for distance relay of line 9-6 at bus 9

For that event tree, the expected path and the real path of relay operations are listed in Table 3.6. Similarly, other local monitoring tools in the system will also generate an event tree analysis. Finally, the system monitoring tool will collect the activity path of each corresponding event tree to see what was going on in the system and decide if the corrective methods are appropriate. Having the detailed local information, a study of the

transient stability can be performed and coordinated with other system considerations to counteract the impact of the disturbance.

Table 3.6 Monitoring of Relay Operations

Relay no.	**Expected path**	**Real path**
Relay 9: event tree 1	*1-2- white*	*1-3-4-white*

3.9 Conclusions

There are two ways to reduce the probability of cascading blackouts at the local substation level: i) Improving real-time fault analysis using better techniques than conventional distance relays. ii) Improving the communications between system-wide and local level to obtain more comprehensive monitoring methods. NNFDC and SSFL are basically derived from two different approaches. The combination of the two algorithms provides a more accurate fault analysis and can double-check the analysis result of the relays. The event tree analysis is easy to realize and it can provide an understanding of the event sequences happening at local sites. That can help system operators make an effective corrective decision quickly. The proposed methods are in accordance with the NERC recommendations and fit well in the trend of the wide area protection and control.

4. Interactive Scheme of System and Local Monitoring and Control

4.1 Interactive Scheme Description and Steps

For the routine security analysis, the system monitoring and control tool obtains power system information from measurements (i.e., SCADA) and runs the vulnerability analysis, as well as static and dynamic contingency analysis. Vulnerability analysis evaluates the vulnerability of individual element and the whole system. Static and dynamic contingency analysis finds the contingencies which can lead to problems such as line overload, bus low/high voltage, angle stability, voltage stability, etc. The emergency control means will be chosen and used to mitigate such expected contingencies. The critical elements, which are more vulnerable to contingencies, or whose outages may threaten the system security, will be found based on the above analysis. This information will be sent to the local monitoring and control tool for detailed monitoring.

The local monitoring and control tool serves as a backup on-line fault analysis tool using a combined NNFDC and SSFL algorithm. When a suspect disturbance is detected, either by relay or by the fault analysis tool, the local analysis tool will find the matching event tree according to the fault analysis result. Then the actual relay operations will be tracked in that event tree and finally the event sequence of that relay system will be obtained. This information will be sent to the system analysis tool for further system security analysis. The misoperations of relays can be corrected by local action quickly or mitigated by system security control after a detailed system-wide analysis.

System event-based analysis will get the disturbance information from system measurements and local tool. If such events are studied by the routine security analysis, pre-determined emergency control means will be activated. If the events are unexpected, transient stability analysis and power flow analysis will be run to see whether there are transient stability or steady state problems. If so, associated control means will be found and issued to mitigate such events. The following is a sequence of the analysis steps:

Step 1: Routine vulnerability and security analysis performed by the system-wide tool: (a) decides security level and finds vulnerable elements, then sends monitoring command to the local tool; (b) identifies critical contingencies, and starts associated control schemes to find the control means for those expected events.

Step 2: Local monitoring performed by the local tool: (a) starts analysis when disturbance occurs; (b) if it finds relay misoperation, it makes correction or receives system control command for better control; (c) reports disturbance information and analysis to the system tool.

Step 3: Event-based security analysis performed by the system tool: (a) if it finds a match with expected event, activates the emergency control; (b) if it does not find a match, analyzes if the system is secure or not; (c) if it is not, finds new emergency control and activates it.

Step 4: Update information and go to Step 1.

4.2 Description of the Block Diagrams

The block diagrams of relationship between the system and local monitoring and control tools are shown in Figure 4.1 and Figure 4.2. An example of field installation is given in Figure 4.3.

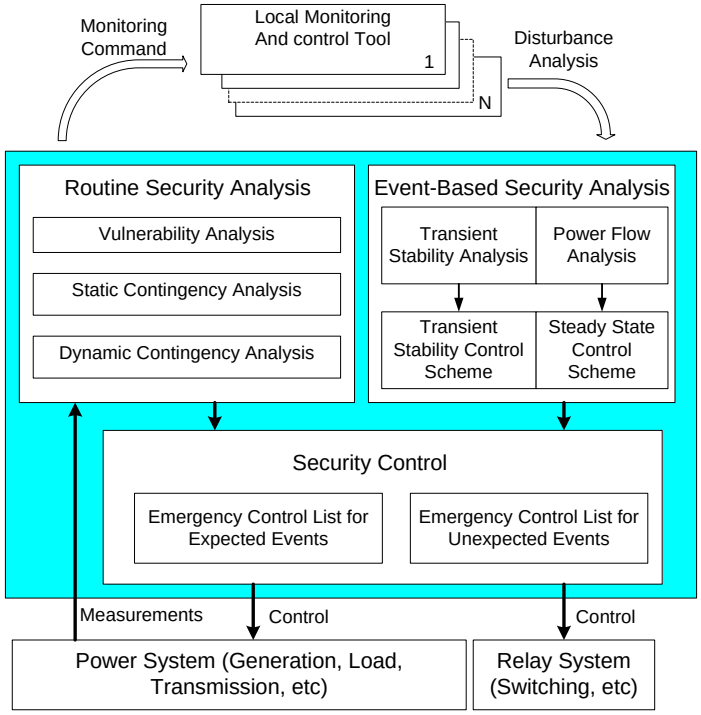

Figure 4.1 Block diagram of system monitoring and control

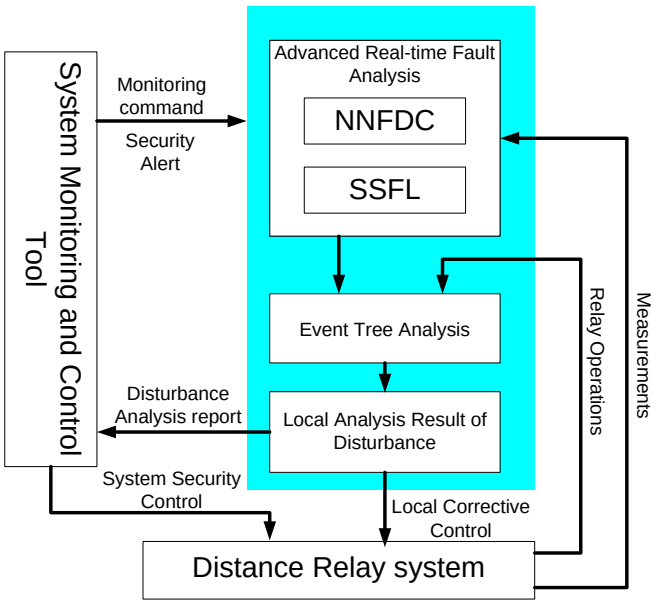

Figure 4.2 Block diagram of local monitoring and control

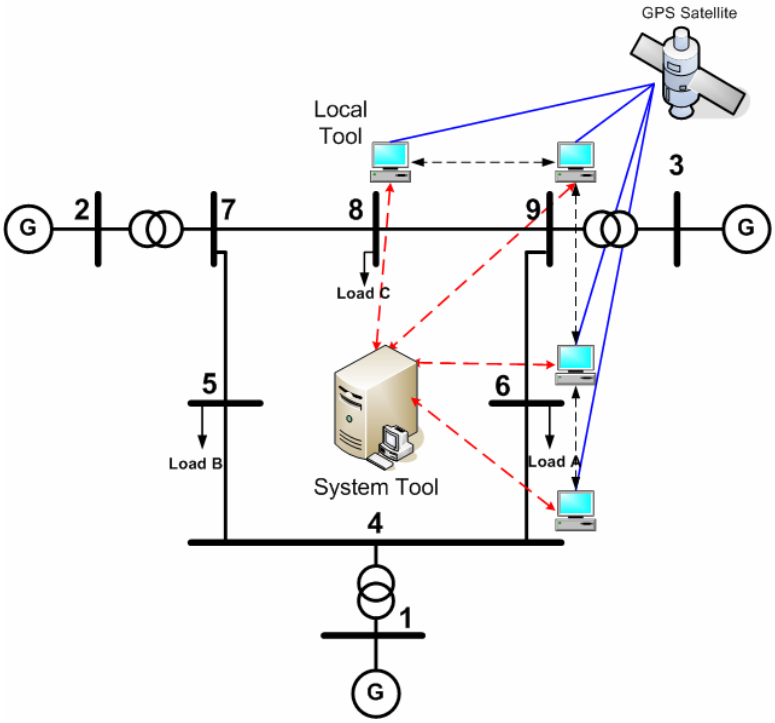

Figure 4.3 An example of field installation

4.3 Case Studies

The IEEE 39-bus New England test system, as shown in Figure 4.4, is used to demonstrate the new approach. Detailed system data can be found in [26].

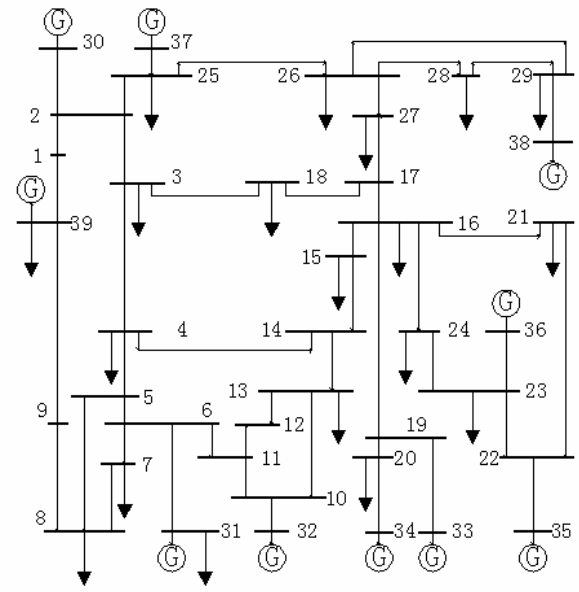

Figure 4.4. IEEE 39-Bus system

Case 1. Routine system security analysis

In this case, the system routine security analysis is implemented off-line and the vulnerable lines in the system are found. For those lines, the local analysis tool proposed in this paper needs to be installed to monitor the relays.

From topology processing, we find 11 lines from the one-line diagram shown in Figure 4.4: L22(B19-16), L47(B20-19), and 9 generator branches L37-L45 which connect G30-G38 respectively. There will be one or several buses isolated from the system if any of the above 11 lines are disconnected. The local analysis tools need to be applied on those lines.

By vulnerability analysis for distance relays (we assume all lines have distance relays), we find the top 6 most vulnerable lines according to their vulnerable indices as shown in Table 4.1. For those lines, the fault on the neighboring lines may affect their relay operations. Therefore, those lines also need to be monitored using the local analysis tools.

Table 4.1 Vulnerable lines and their neighboring lines

Line No	**Bus Connection**	**VI_ Relay**	**Neighboring Lines (the contingency on those lines could influence the vulnerable line)**
L37	B6-31	0.0240	L9(B6-5),L11(B7-6),L12(B11-6)
L38	B10-32	0.0206	L16(B11-10),L17(B13-10)
L42	B23-36	0.0191	L28(B23-22),L29(B24-23)
L45	B29-38	0.0157	L33(B29-26),L34(B29-28)
L43	B25-37	0.0149	L4(B25-2),L30(B26-25),L33
L29	B24-23	0.0131	L24(B24-16),L28,L42

Case 2. Event-based security analysis

In this case, it will be demonstrated how relay misoperation can cause system blackout. Then we describe how to prevent such situation with the benefit of the proposed interactive analysis approach.

The sequence of the scenarios is as follows:

1) t=0s, a 3-phase fault occurs at middle of L27(B22-21).

2) The fault is cleared at t=0.11s by tripping L27.

3) t=1s, a second 3-phase fault occurs at middle of L3(B3-2).

4) The second fault is cleared at t=1.11s by tripping L3.

This contingency may cause relay at B24 of L29 (B24-B23) to misoperate. The trajectory of impedance seen by that relay is shown in Figure 4.5 with the event sequence labeled. The relay sees zone 3 fault at t=0.242s after the first fault clearing till t=1.008s the trajectory

leaves zone 3 circle. Then the relay sees zone 3 fault again at t=1.520s. It may stay at the zone 3 circle longer than the setting time. The distance relay may trip L29 if zone 3 timer expires.

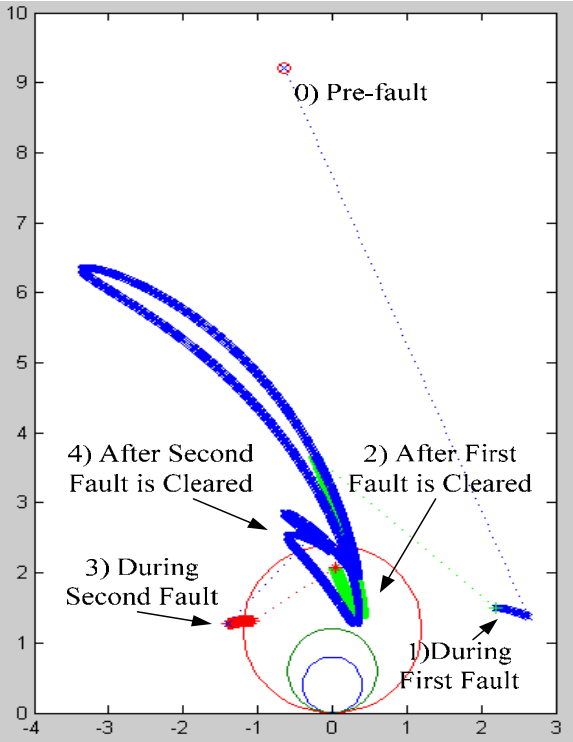

Figure 4.5 Apparent impedance seen by distance relay at L29 (B24-23) during the 4s simulation period

Thus, buses 22, 23, 35 and 36 will be isolated from the system, including the G35, G36 and load at B23, B24. The rest of the system is unbalanced and further cascading outage may happen.

This situation can be prevented by the interactive system and local analysis. From Table 4.1, we can see L29 has already been placed on the vulnerable line list and the local analysis tool needs to be installed on that line. When the first fault occurs, the event-based system security analysis is activated. Through power flow analysis, it is determined that L29 is heavily loaded due to L27 outage. Also from the topology processing, it is determined that L29 and L27 are critical pairs. Therefore, through the system analysis, an alert signal will be sent to the local analysis tool at L29 to increase the security level. When the second fault happens, the local analysis tool draws a conclusion to block the relay from tripping for zone 3 fault. That information will be sent back to the system. The system will issue appropriate control means to mitigate the disturbances.

In an actual large scale system, it is impossible that one or two contingencies like the ones discussed in this scenario can cause large scale system oscillation. Usually there is enough time for coordinating the system-wide and local analysis to mitigate the disturbances before they unfold into the large one. An interactive system-wide and local analysis approach can really help understand the disturbances and improve the security of system operations.

4.4 Conclusions

Following conclusions can be drawn in this section:

- New approach to help detect and prevent cascading outage can be obtained by coordinating the system-wide and local monitoring and control tools.
- The system-wide monitoring and control tool can find the vulnerable elements and send command to the local tool for detailed monitoring.
- Emergency control means for expected events can be found by the routine security analysis and activated when such events occur.
- Emergency control means for unexpected events can be found by event-based security analysis and activated to mitigate the disturbance and to help keep the system secure.
- The local monitoring and control tool can find the exact disturbance information and make a correction if there is relay misoperation. Further information can be sent to the system tool for better security control.
- Further work to solve the application issues is needed to fulfill the task, which is “detection, prevention and mitigation of cascading events”.

5. Conclusions

This final report gives detailed description of the tools and techniques developed by Texas A&M University to help detect, prevent and mitigate cascading events. The interactive scheme of system-wide and local monitoring and control tools can work together with the schemes of wide area measurement based remedial action and adaptive islanding with selective under frequency load shedding to fulfill the project goal: detection, prevention and mitigation of cascading events.

The interactive scheme of system-wide and local monitoring and control tools to help detect and prevent cascading events is proposed and tested.

The system-wide monitoring and control tool includes Network Contribution Factor (NCF) method, Vulnerability Index (VI), Margin Index (MI), contingency analysis (CA), steady state analysis and control (SSAC), transient stability analysis and control (TSAC), static and dynamic relay analysis (RA), etc.

The local monitoring and control tool includes the neural network based fault detection and classification (NNFDC), synchronized sampling based fault location (SSFL), and event tree analysis (ETA). The three techniques combine together as an advanced real time fault analysis tool and relay monitoring tool. Power swing and its influence on the fault analysis are also presented. The performance studies for NNFDC and SSFL show their advantages over the conventional distance relay when dealing with a variety of fault events and system conditions. The case study of the relay monitoring tool shows its effectiveness in providing a graphic view of disturbance information.

The system-wide monitoring and control tool can find the vulnerable elements and send command to the local tool for detailed monitoring. The vulnerability and security margin information can be obtained by Vulnerability Index (VI) and Margin Index (MI) methods. Emergency control approaches for expected events can be found by the routine security analysis and activated when such events occur. Emergency control approaches for unexpected events can be found by event-based security analysis and activated to mitigate the disturbance and keep the system secure.

The local monitoring and control tool can find the exact disturbance information and make a correction if there is relay misoperation. Further information can be sent to the system monitoring and control tool for better security control.

The proposed interactive scheme of system-wide and local monitoring and control is tested using the IEEE 39-bus system. It shows the promising results for the detection and prevention of possible cascading events.

PUBLICATIONS

[1] H. Song, M. Kezunovic, "Relieving Overload and Improving Voltage by the Network Contribution Factor (NCF) Method", NAPS2004, 36th Annual North American Power Symposium, Moscow, Idaho, August, 2004

[2] H. Song, M. Kezunovic, "A Comprehensive Contribution Factor Method for Congestion Management", 2004 IEEE Power Systems Conference & Exposition (PSCE), New York, October, 2004

[3] H. Song, M. Kezunovic, "Stability Control using PEBS method and Analytical Sensitivity of the Transient Energy Margin", 2004 IEEE PES Power Systems Conference & Exposition (PSCE), New York, October, 2004

[4] H. Song, M. Kezunovic, "Static Security Analysis based on Vulnerability Index (VI) and Network Contribution Factor (NCF) Method", 2005 IEEE PES T&D Asia Pacific, Dalian, China, August, 2005

[5] H. Song, M. Kezunovic, "Static Analysis of Vulnerability and Security Margin of the Power System", 2005 IEEE PES T&D Conference, New Orleans, Oct. 2005

[6] N. Zhang, H. Song, M. Kezunovic, "New Monitoring and Control Scheme for Preventing Cascading Outage", NAPS2005, 37th Annual North American Power Symposium, Ames, Iowa, October, 2005

[7] N. Zhang, M. Kezunovic, "Verifying the Protection System Operation Using an Advanced Fault Analysis Tool Combined with the Event Tree Analysis", NAPS2004, 36th Annual North American Power Symposium, Moscow, Idaho, August, 2004

[8] N. Zhang, M. Kezunovic, "A Study of Synchronized Sampling Based Fault Location Algorithm Performance under Power Swing and Out-of-step Conditions", PowerTech 2005, St. Petersburg, Russia, June, 2005

[9] N. Zhang, M. Kezunovic, "Coordinating Fuzzy ART Neural Networks to Improve Transmission Line Fault Detection and Classification", 2005 IEEE PES General Meeting, San Francisco, June, 2005

[10] N. Zhang, M. Kezunovic, "Implementing an Advanced Simulation Tool for Comprehensive Fault Analysis", 2005 IEEE PES T&D Asia & Pacific Conference, Dalian, China, Aug. 2005

[11] N. Zhang, M. Kezunovic, "Improving Real-time Fault Analysis and Validating Relay Operations to Prevent or Mitigate Cascading Blackouts", 2005 IEEE PES T&D Conference, New Orleans, Oct. 2005

REFERENCES

[1] H. Song, M. Kezunovic, "Relieving Overload and Improving Voltage by the Network Contribution Factor (NCF) Method", NAPS2004, 36th Annual North American Power Symposium, Moscow, Idaho, August, 2004

[2] H. Song, M. Kezunovic, "A Comprehensive Contribution Factor Method for Congestion Management", 2004 IEEE Power Systems Conference & Exposition (PSCE), New York, October, 2004

[3] H. Song, M. Kezunovic, "Stability Control using PEBS method and Analytical Sensitivity of the Transient Energy Margin", 2004 IEEE PES Power Systems Conference & Exposition (PSCE), New York, October, 2004

[4] H. Song, M. Kezunovic, "Static Security Analysis based on Vulnerability Index (VI) and Network Contribution Factor (NCF) Method", 2005 IEEE PES T&D Asia Pacific, Dalian, China, August, 2005

[5] H. Song, M. Kezunovic, "Static Analysis of Vulnerability and Security Margin of the Power System", 2005 IEEE PES T&D Conference, New Orleans, Oct. 2005

[6] N. Zhang, H. Song, M. Kezunovic, "New Monitoring and Control Scheme for Preventing Cascading Outage", NAPS2005, 37th Annual North American Power Symposium, Ames, Iowa, October, 2005

[7] N. Zhang, M. Kezunovic, "Verifying the Protection System Operation Using an Advanced Fault Analysis Tool Combined with the Event Tree Analysis", NAPS2004, 36th Annual North American Power Symposium, Moscow, Idaho, August, 2004

[8] N. Zhang, M. Kezunovic, "A Study of Synchronized Sampling Based Fault Location Algorithm Performance under Power Swing and Out-of-step Conditions", PowerTech 2005, St. Petersburg, Russia, June, 2005

[9] N. Zhang, M. Kezunovic, "Coordinating Fuzzy ART Neural Networks to Improve Transmission Line Fault Detection and Classification", 2005 IEEE PES General Meeting, San Francisco, June, 2005

[10] N. Zhang, M. Kezunovic, "Implementing an Advanced Simulation Tool for Comprehensive Fault Analysis", 2005 IEEE PES T&D Aisa & Pacific Conference, Dalian, China, Aug. 2005

[11] N. Zhang, M. Kezunovic, "Improving Real-time Fault Analysis and Validating Relay Operations to Prevent or Mitigate Cascading Blackouts", 2005 IEEE PES T&D Conference, New Orleans, Oct. 2005

[12] U.S.-Canada Power System Outage Task Force, "Final Report on the August 14, 2003 Blackout in the United States and Canada: Causes and Recommendations", April 5, 2004, Available: http://www.nerc.com

[13] NERC System Disturbances Reports, North American Electric Reliability Council, New Jersey, 1984-1991

[14] NERC Disturbance Analysis Working Group, “Western Interconnection (WSCC) System Disturbance — August 10, 1996”, *NERC 1996 System Disturbances Report*, Aug 2002, Available: http:// www.nerc.com

[15] Q. Chen, K. Zhu, J.D. McCalley, "Dynamic decision-event trees for rapid response to unfolding events in bulk transmission systems", in Proc. of IEEE 2001 Power Tech Proceedings, Vol. 2 , Sept 2001

[16] B.A. Carreras, V.E. Lynch, I. Dobson, "Dynamical and probabilistic approaches to the study of blackout vulnerability of the power transmission grid", in 2004 Proc. of the 37th Annual Hawaii International Conference on System Sciences, Jan. 2004, pp. 55 - 61

[17] J.C. Tan, P.A. Crossley, P.G. McLaren, "Application of a wide area backup protection expert system to prevent cascading outages", *IEEE Transactions on Power Delivery*, vol. 17(2), April 2002, pp. 375 - 380

[18] D. C. Elizondo, J. de La Ree, A. G. Phadke, S. Horowitz, “Hidden failures in protection systems and their impact on wide-area disturbances”, in *Proc. of IEEE 2001 PES Winter Meeting*, Jan/Feb 2001, Vol. 2, pp. 710 – 714

[19] M. Larsson, C. Rehtanz, J. Bertsch, “Monitoring and operation of transmission corridors”, in *2003 IEEE Power Tech Conference Proceedings*, vol. 3, June 2003

[20] P. Kundur, *Power System Stability and Control*, New York, McGraw-Hill, Inc., 1993

[21] H.-D. Chiang, F.F. Wu, P.P. Varaiya, “Foundations of the potential energy boundary surface method for power system transient stability analysis”, *IEEE Trans. Circuits and Systems*, vol. 35(6), pp. 712 - 728, June 1988.

[22] M. Pavella, P. G. Murthy, *Transient Stability of Power Systems, Theory and Practice*, New York: J.WILEY & SONS, 1994.

[23] P. Omahen, “Fast transient stability assessment using corrective PEBS method”, in Proc. 1991 6th Mediterranean Electrotechnical Conference, vol.2, pp.1408 – 1411.

[24] B. Stott, O. Alsac, “Fast Decoupled Load Flow”, *IEEE Trans. Power Apparatus and Systems*, vol. 93, pp. 859 – 869, 1974.

[25] V. Chadalavada, V. Vittal, “Transient stability assessment for network topology changes: application of energy margin analytical sensitivity”, *IEEE Trans. Power Systems*, vol. 9(3), pp. 1658 –1664, Aug 1994

[26] M. A. Pai, Energy Function Analysis for Power System Stability, Kluwer Academic Publishers, Norwell, MA, 1989, pp.222-227

[27] NERC Disturbance Reports, North American Electric Reliability Council, New Jersey, 1996-2001.

[28] A. G. Phadke, J. S. Thorp, “Expose hidden failures to prevent cascading outages” , Computer Applications in Power, IEEE , Vol. 9 , No. 3 , pp. 20-23, July 1996.

[29] Wide Area Protection and Emergency control, Final Report, Working Group C-6, System Protection Subcommittee , IEEE Power System Relaying Committee

[30] S. Vasilic, M. Kezunovic, "Fuzzy ART neural network algorithm for classifying the power system faults," *IEEE Trans. on Power Delivery*, vol. 20, no. 2, pp.1306-1314, April 2005.

[31] G. A. Carpenter and S. Grossberg, "ART2: self-organization of stable category recognition codes for analog input patterns", *Applied Optics*, vol. 26, no. 23, pp. 4919-4930, Dec. 1987.

[32] J. Keller, M. R. Gary, and J. A. Givens: "A fuzzy k-nearest neighbor algorithm", *IEEE Trans. Systems, Man and Cybernetics*, vol. 15, no. 4, pp. 580-585, Jul./Aug. 1985.

[33] Slavko Vasilic, M. Kezunovic, Dejan Sobajic, "Optimizing performance of a transmission line relaying algorithm implemented using an adaptive self-organized neural network," *14th Power Systems Computation Conference '02*, Seville, Spain, June 2002.

[34] M. Kezunovic, B. Perunicic, "Automated Transmission Line Fault Analysis Using Synchronized Sampling at Two Ends," *IEEE Trans. on Power Systems*, Vol. 11, No. 1, pp. 441-447, Feb. 1996.

[35] A. Gopalakrishnan, M. Kezunovic, S.M. McKenna, D.M. Hamai, "Fault Location Using Distributed Parameter Transmission Line Model," *IEEE Trans. on Power Delivery* Vol. 15, No. 4, pp. 1169-1174, Oct. 2000.

[36] M. Kezunovic, B. Perunicic, and J. Mrkic, "An Accurate Fault Location Algorithm Using Synchronized Sampling," *Electric Power Systems Research Journal*, Vol. 29, No. 3, pp. 161-169, May 1994.

[37] *IEEE standard for synchrophasors for power systems*, IEEE Standard 1344-1995 (R2001), 2001

[38] *IEEE standard Common Format for Transient Data Exchange (COMTRADE) for power systems*, IEEE Standard C37.111-1999, 15 Oct. 1999.

[39] J. D. Andrews, S. J. Dunnett, "Event-tree analysis using binary decision diagrams", *Reliability, IEEE Transactions on*, Vol. 49, No. 2, pp. 230 – 238, Jun. 2000.

[40] Jacobs Sverdrup Inc, System Safety and Risk Management Guide for Engineering Educators: lesson 9 - event tree analysis, [On-line]. Available: http://www.sverdrup.com/safety/riskmgt/lesson_9.pdf

[41] Qiming Chen; Kun Zhu; McCalley, J.D.; "Dynamic decision-event trees for rapid response to unfolding events in bulk transmission systems," in *Proc. of the IEEE Power Tech Conference*, Porto, Portugal, Sept. 2001.

[42] Demetrios Tziouvaras, Daqing Hou, "Out-of-Step Protection Fundamentals and Advancements", 30th Annual Western Protective Relay Conference, October 21-23, 2003, Spokane, Washington.

[43] CanAm EMTP User Group, *Alternative Transient Program (ATP) Rule Book*, Portland, 1992.

[44] The MathWorks, Inc., *Using MATLAB*, Natick, Jul. 2002.

[45] D. Ristanovic, S. Vasilic, M. Kezunovic, "Design and implementation of scenarios for evaluating and testing distance relays," North American Power Symposium - NAPS, College Station, Texas, Oct. 2001.

[46] P. M. Anderson, A. A. Fouad, *Power System Control and Stability,* vol. I. The Iowa State University Press, Ames, Iowa, 1977, p. 38.

[47] S. Vasilic, "Fuzzy neural network pattern recognition algorithm for classification of the events in power system networks," Ph.D. dissertation, Dept. Electrical Eng., Texas A&M University, College Station, Texas, May 2004.

[48] W. A. Lewis and S. Tippet, "Fundamental basis for distance relaying on 3-phase systems," *AIEE Trans*., vol. 66, pp. 694–708, Feb. 1947.

[49] SEL-321 Phase and Ground Distance Relay, Directional Overcurrent Relay, Fault Locator: Instruction Manual, Schweitzer Engineering Laboratories Inc., Pullman, WA, Mar. 1998.